

東京大学 大学院新領域創成科学研究科
基盤科学研究系
先端エネルギー工学専攻

平成 25 年度

修士論文

Development of a Ti-Taper Reed Valve for
Microwave Rocket and Effect on Its Thrust Performance

— マイクロ波ロケットのチタンテーパリードバルブの
開発と推力性能に対する効果 —

2014 年 1 月提出
指導教員 小紫 公也 教授

47126030 栗田 哲志

Acknowledgement

I would like to express my deep gratitude to Professor Kimiya Komurasaki who gave me this worthwhile research theme and many pithy advices. His comment made my research motivation galvanizing. Moreover, he prepared research environment for me and made a lot of opportunities for conference. Without his instruction, my thesis could never be completed.

I am deeply grateful to Associate Professor Koizumi. He gave me ingoing advices. Especially, the design of new reed valve could have never realized without his comments.

Dr. Keishi Sakamoto (Plasma Heating Laboratory, Naka fusion research center, Japan Atomic energy Agency) gave our group the most precious experiment opportunities. Thanks to his attention to provide the experiment opportunity, I got a lot of significant data.

Gratitude is extended to Dr. Koji Takahashi and Dr. Ken Kajiwara who gave me useful and instructive advices. The gratitude is also extended to all members in Plasma Heating Laboratory who gave me warm support for conducting the experiment. Among then, Mr. Yukiharu Ikeda and Mr Shinji Komori helped me a lot including the preparation for the experiments (setups, instruments, etc.)

The experiment could never be successful and my thesis could never be finished without Dr. Yasuhisa Oda. He gave me the experiment direction and instructive advices. Through these instructions, my way of thinking greatly improved. Therefore I would like to express my gratitude to him.

I am grateful to Mr. Toshikazu Yamaguchi and Mr. Masafumi Fukunari. They always supported me a lot as the closest adviser for me. They gave me not only a lot of advices but also the way of thinking to data. From them, I learned a lot of things, preparation for the experiments, treat of experimental instruments. Besides, I have never made my experiment without experimental system Mr. Fukunari made.

I would also like to thank you to all members in Komurasaki-Koizumi lab, especially to Mr. Kenta Asai and Nat Wongsuryrat who gave me a lot of chances to make a discussion as the same research group. Mr. Kenta Asai gave me a lot of advices to analyzing the data, research direction and warm words.

Finally, I would like to express my gratitude to my family. Without their supports, the success of my research and my growth could never be realized.

Contents

Nomenclature

Chapter 1 Research Background

1.1	Actual state of Space Transportation System	1
1.2	Beamed Energy Propulsion (BEP)	2
1.2.1	Research Process of Laser Propulsion System	3
1.2.2	Microwave Rocket and Engine Cycle	3

Chapter 2 Design of thruster

2.1	Refilling effect for Microwave Rocket	6
2.2	Thruster Design	10
2.3	Design of Reed Valve	16

Chapter 3 Effect of Ti-Taper Reed Valve and Thrust Performance

3.1	Thrust Parameter of Microwave Rocket	24
3.2	Objective of This Experiment	27
3.3	Experimental Apparatus	28
3.3.1	Experimental System	28
3.3.2	Measurement System	32
3.4	Result of Experiment	35
3.4.1	Effect of Reed Valve	35
3.4.2	Relationship between Thrust and Duty Ratio	39

Chapter 4 Conclusion

4.1	Improvement of Refilling Performance by Ti-Taper Reed Valve	48
4.2	Anomalous Ignition and Design Guide of Future Thruster	48

	References	49
--	------------	----

Nomenclature

A	: Area [m^2]
A_s	: Effective area [m^2]
A_{reed}	: Opening area of reed valve [m^2]
b	: Width [mm]
C_m	: Momentum coupling coefficient [N/MW]
D_1	: Inside diameter of the screw [mm]
d_2	: Effective diameter [mm]
E	: Young's modulus of Ti [GPa]
f	: Repetitive pulse frequency [Hz]
f_{safety}	: Safety factor
F	: Thrust [Hz]
I_z	: Second moment of area [m^4]
I	: Impulse [Ns]
L	: Length [mm]
L_{screw}	: Screw length [mm]
l_{hole}	: Length of hole [mm]
l	: Normalized plasma length
\dot{m}	: Mass flow [kg/s]
M_{Max}	: Maximum moment [Nm]
n	: The number of holes for screws
p	: Pressure [Pa]
Δp	: Negative pressure [Pa]
P_0	: Pressure in normal atmospheric pressure [Pa]
P_{peak}	: Input peak power of microwave beam [kW]
P	: Pitch [mm]
r	: Inside diameter [mm]
t	: Thickness of reed valve [mm]
t_{min}	: Minimum thickness [MPa]
u	: Velocity [m/s]
U_{ioniz}	: Propagation velocity of ionization front [m/s]
W	: Load [MPa]
y_0	: Distance between centroid and external diameter [mm]

y_1	: Distance between centroid and inside diameter [mm]
y_{MAX}	: Maximum displacement [mm]
z	: The number of thread ridges
α	: Angle of screw [°]
γ	: Ratio of specific heat
ρ	: Density [kg/m^3]
ρ_0	: Density in normal atmospheric pressure [kg/m^3]
σ_{acryl}	: Allowable stress of acryl [MPa]
σ_c	: Maximum compressive stress [MPa]
σ_{MAX}	: Maximum stress [MPa]
σ_t	: Maximum tensile stress [MPa]
σ_Y	: Yield stress [MPa]
τ	: Pulse duration time [s]
τ_a	: Shear stress of aluminum screw [MPa]

Chapter 1

Research Background

1.1 Actual state of Space Transportation System

In the past, the technology of space transportation system had made a progress. But the present cost of rocket launch is high yet and Space Shuttle retired due to high launch cost. On the other hand, space mission such as ISS (International Space Station) experiment and SSPS (Space Solar Power System and so on) is important in the future. Therefore low cost launch transportation system intended for large mass is required rather than high cost space transportation system intended for human.

Present transportation systems are limited to chemical launch rockets which require huge costs and rocket fuel occupied about 90 % of total weight of the rocket. For example, it costs around 10 billion yen to launch a typical satellite to GTO (Geostationary Transfer Orbit) [1]. There are mainly three reasons for these high costs.

Firstly, chemical rocket systems require huge amount of propellant on board. As stated before, about 90% of typical chemical rocket mass are occupied by fuel and oxidizer [2]. This occurs because the rocket has to carry the propellant. Therefore, achievable payload ratio of a chemical launcher rocket is limited about several percent. Moreover, high weight requires the rocket to produce huge thrust in order to launch itself. To achieve this, the chemical rocket uses propellant in a low-efficient way which causes small specific impulse. Furthermore, once the incident (for instance, air breakup, engine trouble and so on) is occurred, cost damage is enormous.

Secondly, in chemical propulsion, there are many devices on board. One of the representative examples is the turbopump system. It is necessary system to pump the propellant which is added additional pressure. Since almost devices are connected to each other by pipes, huge trouble would happen even if there are immaterial breakdown. In short, each device used in chemical rocket will be expensive and complex.

Finally, a typical chemical rocket is a non-reusable system. As mentioned in the second aspect, manufacturing cost of rocket is quite expensive. Space Shuttle is reusable rocket. But its manufacturing cost is higher than a disposable rocket like typical chemical rocket.

As above stated, the costs for a launch by a chemical rocket are quite high. However, there is a strong demand for low-cost mass transportation systems to space such as the Space Solar Power System (SSPS) project [3]. In order to develop technology like SSPS, low cost rocket and mass transportation system is requisite. Under present circumstance, it is said that the launch cost has to be reduced two-orders to realize SSPS. As one of the possible solution, Beamed Energy Propulsion

(BEP) was suggested.

1.2 Beamed Energy Propulsion (BEP)

Beamed energy propulsion is a propulsion system for which propulsive energy is supplied from outside by high-power beamed electromagnetic wave. The beam source is usually a high-power laser or microwave oscillator on the ground. Fig.1.1 shows conceptual schematic of BEP. In BEP, thrust is obtained by high-pressure gas generated by an irradiated beam from outside.

There are two prospective systems of BEP, which are Laser Propulsion and Microwave Rocket. Both of them utilize atmospheric air as propellant. Presently, the cost of microwave generator is two-orders lower than that of laser generator. BEP has main 3 characteristics. First, its propulsion system is air-breathing system. In short, atmospheric air can be utilized as propellant in these systems because high pressure is generated due to breakdown inside the thruster. For this reason, the amount of propellant on board can be much smaller than typical chemical propulsion systems. Because of this, air-breathing system associate with high payload ratio and low cost.

Secondly, it can use pulse detonation to generate high pressure. That is to say, the compressor is not necessary in these systems like turbopump. Especially, Microwave Rocket only consists of the thruster body, intake, taper which is for focusing electromagnetic wave and reed valves for refilling. Therefore, manufacturing cost is dramatically lower than a chemical propulsion system. In parallel, it is possible that the number of launch is increased because BEP vehicle is easy to manufacture.

Thirdly, the most important devices to generate thrust can be located on the ground. It relates to reutilization and easy maintenance.

For these reasons, BEP are thought to be future low-cost mass transportation system to space.

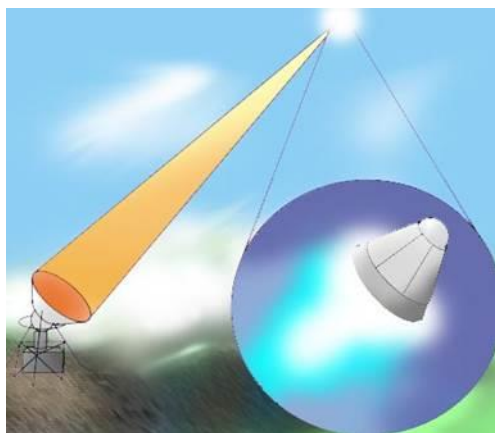


Figure 1.1. Conceptual Schematic of BEP Launch

1.2.1 Research Process of Laser Propulsion System

The concept of Laser Propulsion was first proposed by Kantrowitz in 1972 [4]. Next, Raizer et al revealed that Laser Supported Combustion and Laser Supported Detonation [5]. Moreover, Myrabo et al. conducted a famous launch experiment using a small thruster model named “Light Craft” in 2000 [6]. In the demonstration, the thruster reached 71 m altitude. In 2004, Katsurayama et al. analytically estimated the feasibility of RP Laser Propulsion as SSTO (Single Stage to Orbit) system. In that research, three flight modes were proposed. Those are Pulsejet mode, Ramjet mode and Rocket mode. In pulsejet mode and ramjet mode, propellant is not necessary by utilizing atmospheric air. Hence, it was found that the total cost of Laser Propulsion System is quite lower than that of chemical propulsion system. [7][8][9].

1.2.2 Microwave Rocket and Its Engine Cycle

Microwave Rocket is future transportation vehicle using BEP system. Microwave Rocket can realize low cost because it can use the atmospheric air as a propellant and pulse detonation to generate high pressure. In addition, the beam source can be located on the ground. Fig.1.2 shows the schematic of Microwave Rocket. This rocket takes in fresh air from reed valve and open end during engine cycle. Furthermore, microwave is focused by taper attached at open end of the thruster. The engine cycle of Microwave Rocket is presented in Fig.1.3. The analogy of Pulse Detonation Engine (PDE) cycle is often used to explain this cycle [10]. First, the cycle begins with breakdown in the air by focusing the high-power microwave beam pulse generated. During microwave irradiation, shock wave and ionization front propagate to the open end of the thruster and are exhausted there. This process is called Microwave Detonation. Microwave Rocket acquires the thrust in this instant by the counteraction of high pressure gas. After Microwave Detonation, expansion wave propagates from the open end to the closed end. At this time the inside pressure decreases by the expansion wave and Microwave Rocket starts refilling with fresh air and reed valve is open. Finally, this rocket prepares for the next cycle which begins with the next pulse. Moreover, Microwave Rocket uses microwave oscillator gyrotron on the ground. Gyrotron is developed for International Thermonuclear Experiment Reactor (ITER). There are main three characteristics. It has 170 GHz band, 1 MW power and can oscillate from 0.1 msec and 1000 sec. It has also energy recovery system by Single-Stage Depressed Collector (SDC) and achieved 50 % energy conversion efficiency. Microwave (beam waist: 20.4 mm, Gaussian beam) is outputted by gyrotoron [11][12]. Fig.1.4 shows schematic of gyrotoron. Compared to Laser Propulsion System, Microwave Rocket gains ascendancy over laser propulsion system in terms of the existence of gyrotoron.

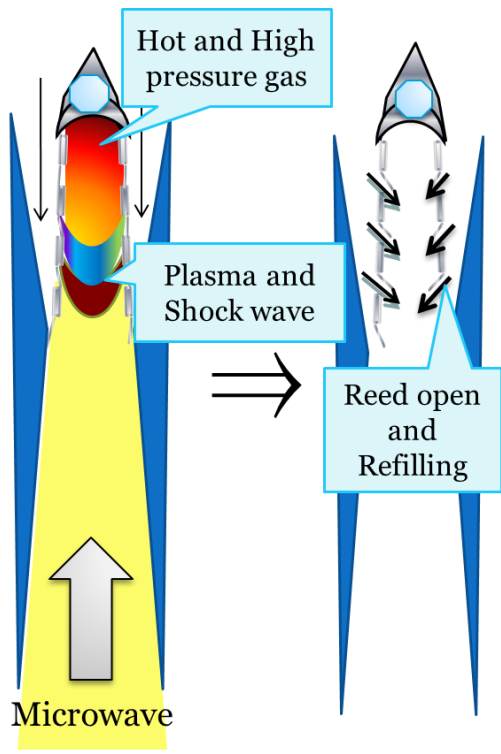


Figure 1.2. Conceptual Schematic of Microwave Rocket

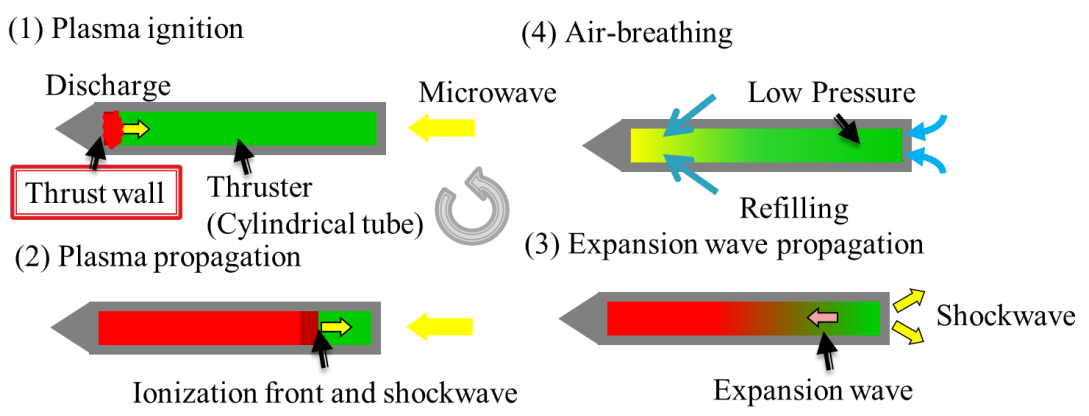


Figure 1.3. Engine Cycle of Microwave Rocket



Figure 1.4. Schematic of a Gyrotron

Table 1.1. Specifications of a Gyrotron

Frequency	170GHz
Output Power P	< 1MW
Beam Profile	Gaussian
Beam waist	40mm
Electrical efficiency	60%

Chapter 2

Design of the Thruster

2.1 Refilling effect for Microwave Rocket

As mentioned above, fresh air is needed inside the thruster for Microwave Rocket. However, the thrust of Microwave Rocket is decreased in case of multi pulse operation because hot and expansive gas remains between pulse and pulse. Because of this, Shiraishi et al conducted the experiment using a thruster which has forced air-breathing system. Its thruster is filled at all times by fresh air. Fig.2.1. shows experimental result in comparison to normal thruster and the thruster which has forced air-breathing system.

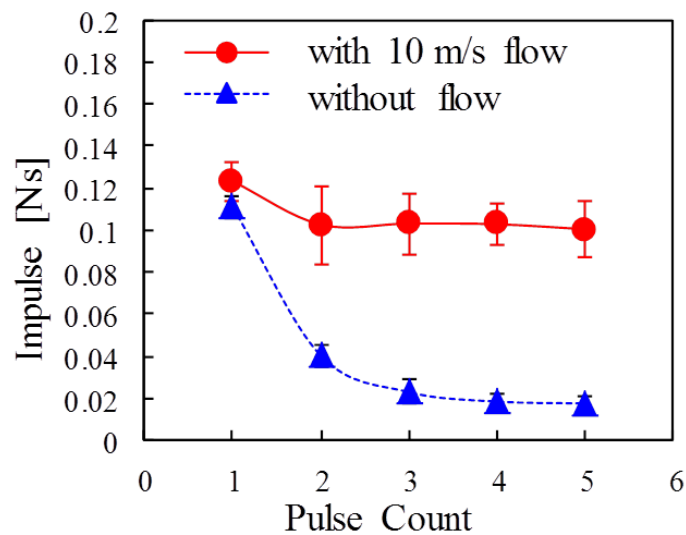


Figure 2.1. Thrust Impulse for Each Pulse Count in Repetitive Pulse Operations.

Reprinted from [13]

It was shown that thrust decrement was prevented due to making an improvement of refilling. Although forced air-breathing system has high efficiency to the thrust, the system is quite complex and needs vacuum chamber. Therefore, Komatsu et al studied reed valve air-breathing system. It was found that its system was simple and corresponded to pressure oscillation [14].

Impulse generated between engine cycles is obtained for the product of plateau pressure, plateau pressure time and area of closed end. Fig.2.2 shows pressure history and microwave signal at closed end. A is area of closed end. From impulse equation of Fig.2.2, it can be said that efficiency of

preventing the plateau pressure decrement corresponds that of preventing the thrust decrement. Fig.2.3 shows picture image of old thruster. The thruster was made from tube, reed valve attachment and collector. Only data of pressure history is acquired from this thruster. In order to get a lot of data, the thruster which can be measured about some data (for example plasma propagation, shockwave velocity, thrust) is needed for next thruster. Moreover the weight of old thruster is about 700 g. The thruster is unsuited for vertical launch. Saitoh et al conducted the vertical launch experiment by using the old thruster. Fig.2.4. shows relationship between normalized plateau pressure and repetitive pulse frequency. If there is no thrust decrement between multi pulse operations, normalized plateau pressure is unity. It was shown that reed valve air-breathing system has an efficiency of preventing the plateau pressure decrement in large repetitive pulse frequency. Nevertheless, difference of normalized plateau pressure was small. Because of this, refilling volume is needed further for Microwave Rocket.

Next, problem of old reed valve is considered. In past study, reed valve (material: SUS304CSP, length: 27.5 mm, width: 12 mm, thickness: 0.2 mm) was used in the experiment. Fig.2.5 shows reed valve. The Impulse was verified using reed valve. In that experiment, reed valve was overstressed and plastic deformation was occurred. Therefore, leak of high pressure generated in engine cycle was occurred and impulse was decreased. Fig.2.6. shows impulse decrement due to plastic deformation [15].

Considering these experiment result, design guideline of the thruster and reed valve was decided. First, a thruster which integrates reed valve attachment into the tube is needed to decrease the thruster weight for vertical launch. Second, reed valve which can open widely and has tough body has to be made to increase the refilling volume and prevent the plateau pressure decrement and therefore the thrust decrement. Third, window for observing plasma is needed for next thruster.

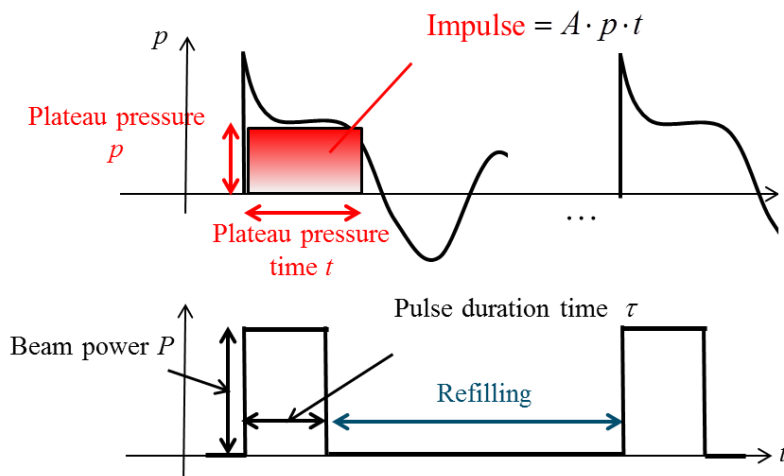


Figure 2.2. Pressure History and Microwave Signal at Closed End of the Thruster

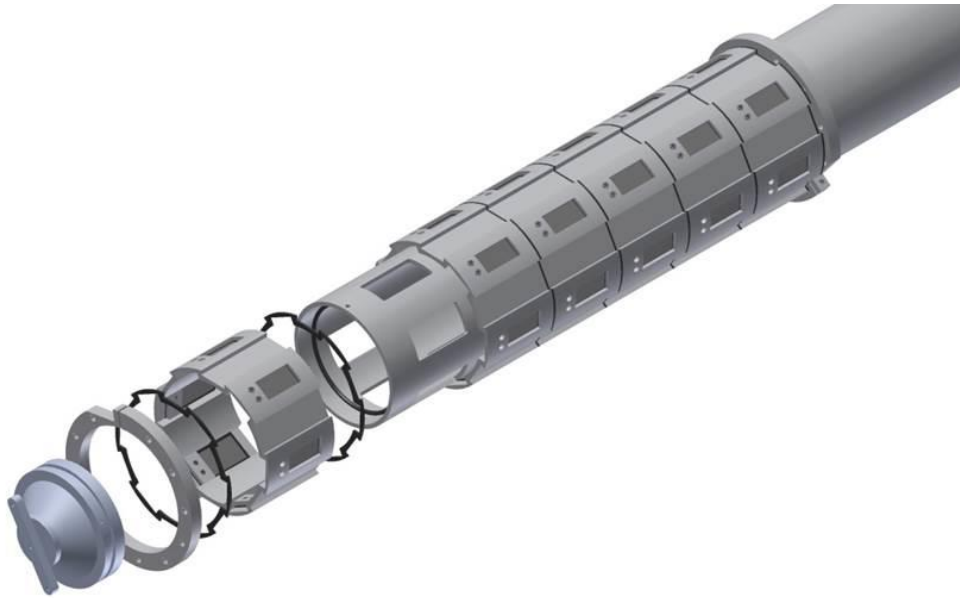


Figure 2.3. Picture Image of Old Thruster

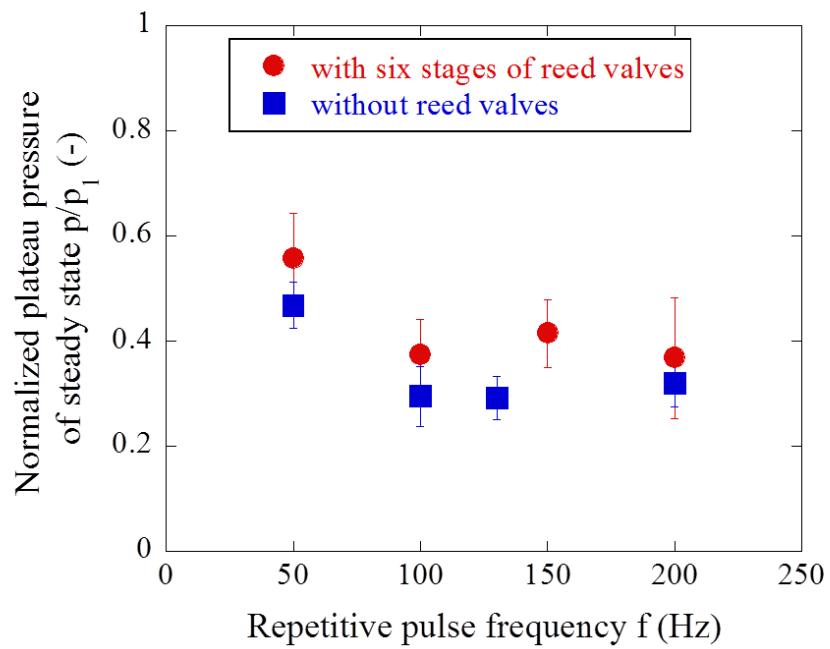
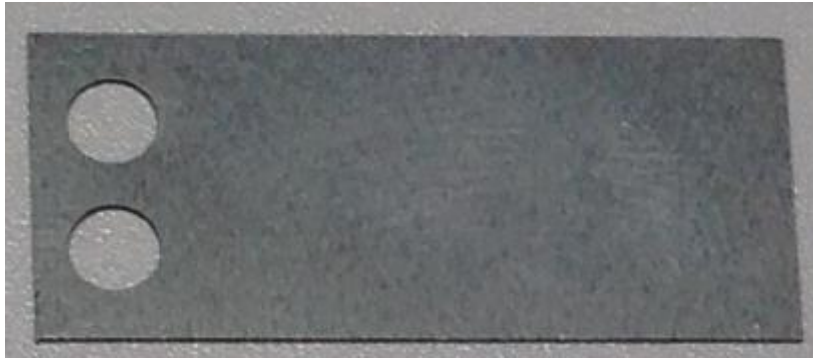


Figure 2.4. Relationship between Normalized Plateau Pressure and Repetitive Pulse Frequency



Material	: SUS304CSP
Length	: 27.5 mm
Width	: 12 mm
Thickness	: 0.2 mm, 0.3 mm

Figure 2.5. Reed Valve used in Past Experiment

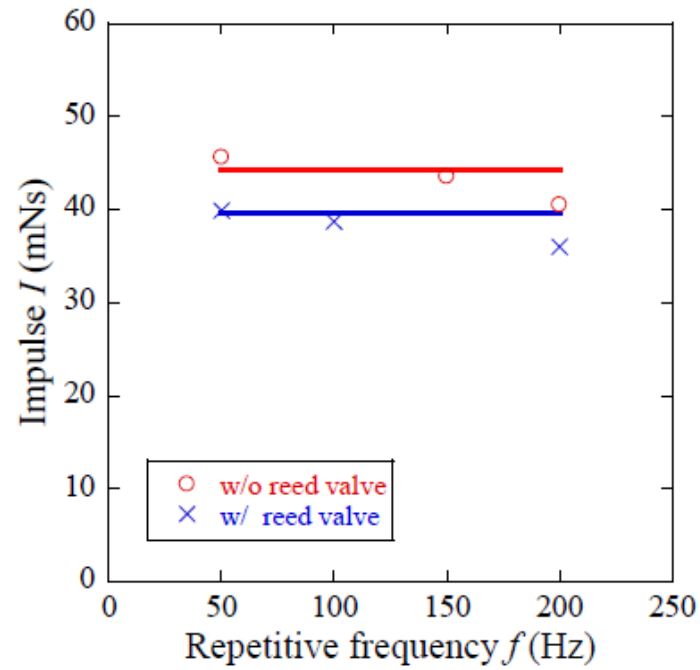


Figure 2.6. Impulse Decrement due to Plastic Deformation. Reprinted from [15]

2.2 Thruster Design

From past study, it was said that cylinder shape is better as the thruster of Microwave Rocket because microwave beam of long pulse duration time is irradiated by gyrotron and microwave has longer wave length than laser. Based on this, new thruster was designed. First of all, light vehicle is important not only chemical propulsion rocket but also Microwave Rocket. Therefore, aluminum (A5056) was selected as the material of Microwave Rocket. Because high pressure is generated during engine cycle, maximum plateau pressure was estimated. In past vertical launch experiment (December 2012), maximum plateau pressure 0.35 Pa was derived. Cylinder thickness of the thruster was calculated by using that figure. Calculating formula is following. Yield stress of A5056 is 98 MPa and inside diameter is 56 mm to compare the past result. Moreover, factor of safety is 1.2. From this calculation, it was shown that over 0.12 mm thickness is needed.

$$t_{\min} = \frac{r}{\sigma_Y / f_{\text{safety}}} p \cong 0.12 \text{mm} \quad (1)$$

t_{\min}	:	Minimum thickness
r	:	Inside diameter
σ_Y	:	Yield stress of A5056
f_{safety}	:	Factor of safety

Integrating reed valve attachment and the tube is needed for new thruster. Therefore, we decided that the inside diameter is 56 mm and external diameter 65 mm. to attach reed valve like inner moat . Fig.2.7. shows picture of new thruster. Like this, new thruster has screw feature both sides and is assembled by connecting the thruster. Moreover, considered air leakage efficiency, thruster has two stage series of reed valves. Although old thruster has six holes for reed valve, the number of the holes is needed to attach for increasing refilling volume. Hence, intensity of holes distance was calculated. The calculating formula is following. Both ends supported beam was considered for proximate calculation and the model of proximate cross-section convex model. Fig.2.8 and Fig.2.9 shows proximate calculation model.

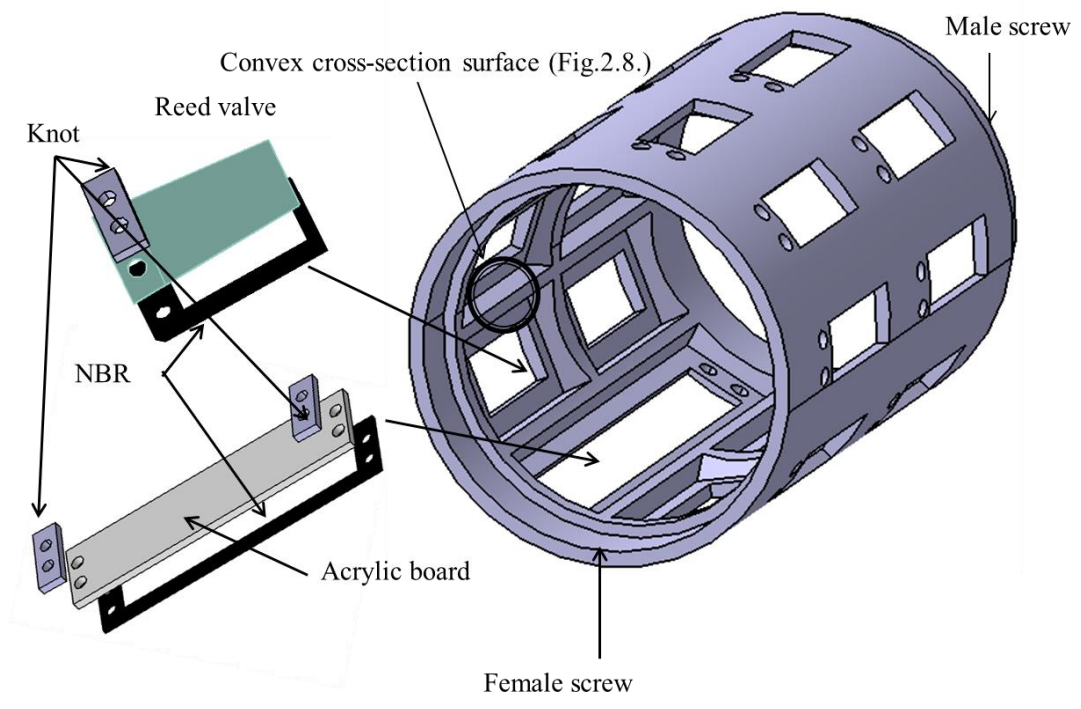


Figure 2.7. Image of New Thruster with Reed Valve

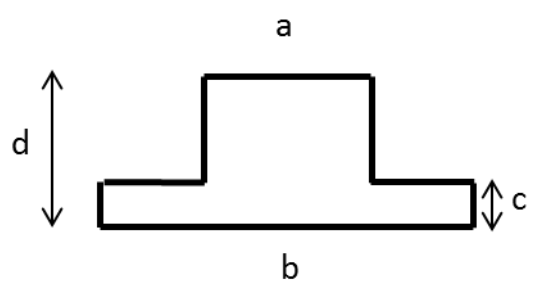


Figure 2.8. Proximate Cross-Section between the Holes of Reed Valves

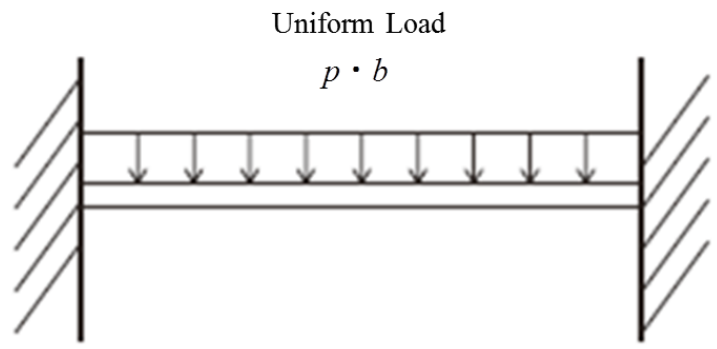


Figure 2.9. Schematic of Both Ends Supported Beam

$$A = a(d - c) + bc$$

$$y_0 = \frac{1}{A} \int_A y dA, y_1 = d - y_0$$

$$I_z = \int_A y^2 dA$$

$$M_{MAX} = \frac{(p \cdot b) \cdot l^2}{24}$$

$$\therefore \sigma_t = \frac{M_{MAX}}{I_z / y_0} \cong 1.17 MPa, \sigma_c = \frac{M_{MAX}}{I_z / y_1} \cong 2.15 MPa$$

A	: Area
y_0	: Distance between centroid and external diameter
y_1	: Distance between centroid and inside diameter
I_z	: Moment of inertia of area
M_{MAX}	: Maximum moment
p	: Pressure
l	: Length of hole
σ_t	: Maximum tensile stress
σ_c	: Maximum compressive stress

This calculation was conducted as there are 9 holes on the same circumference. The formula is above. Because both stresses are under yield stress of A5056, it was decided that the number of holes for reed valve was 9.

Next, the window for plasma observation is considered. Because there are 9 holes for reed valve, it was decided that one of the holes is for plasma observation. The material of window is acryl because it is cheap and light. Although resistance temperature to heat of normal acryl is from 70 to 90, heating time is under 1 second and transformation has never seen in past experiment. The thickness of acryl was also calculated not to be broken down during the experiment. Calculation model is both ends supported beam in a similar way of reed valve hole. Calculation formula is following. Fig.2.10 shows relationship between stress and thickness of acryl using following formula. From Fig.2.10, thickness of 2 mm suffices as acrylic window.

$$\sigma_{acryl} = \frac{\sigma_Y}{f} = \frac{71}{1.3} \cong 54.62MPa$$

$$\sigma = \frac{M}{bt^2/6}$$

σ_{acryl}	: Allowable stress of acryl
σ_Y	: Yield stress of acryl
σ	: Maximum stress of acryl
b	: Width of acryl
t	: Thickness of acryl

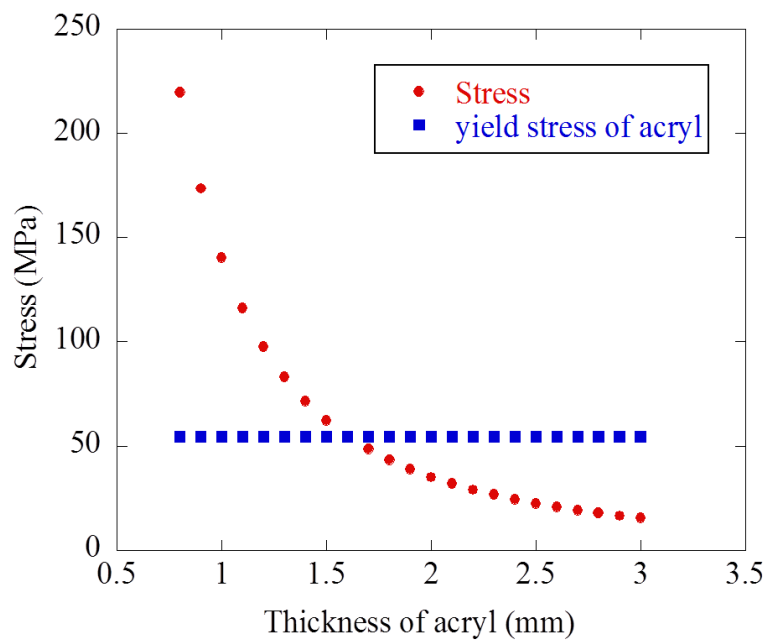


Figure 2.10. Relationship between Stress and Thickness of Acryl

Next, the tube which is connected to the thruster has reed valve was designed. This part has to have acrylic window for plasma propagation. In order to compare past result, the length of this part was decided so that total length of the thruster was 500 mm. The thickness is 0.8 mm from equation (1). Fig.2.11 shows assembling image of this part. Nitrile butadiene rubber (NBR) was used for air leakage efficiency between the tube and acryl. The size of screw and effective depth for fixing the acrylic window was calculated. Calculating formula is following. In this case, there are three holes for plasma observation and 18 holes for screws.

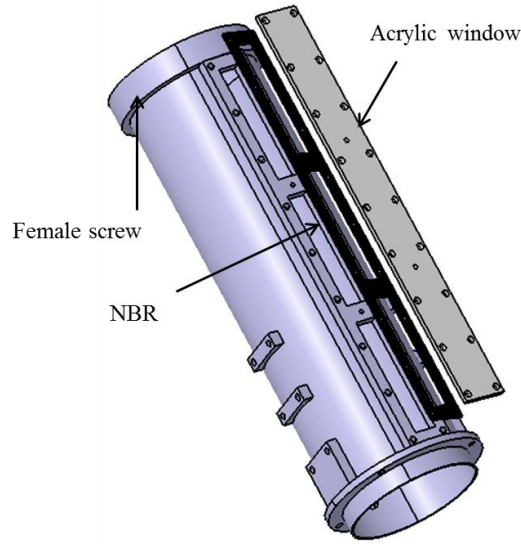


Figure 2.11. Assembling Image of the Acryl

$$A_s = \frac{W}{\sigma_Y}$$

$$\Leftrightarrow A_s = \frac{p \cdot b l_{hole} \cdot 3}{\sigma_Y \cdot n} \cong 0.42 mm^2$$

W	: Load
σ_Y	: Yield stress of aluminum
A_s	: Effective area
p	: Pressure
b	: Width of hole for plasma observation
l_{hole}	: length of hole for plasma observation
n	: The number of holes for screws

From this calculation, effective area is needed over 0.42 for the screw. Because M3 screw has 5.05 effective area, M3 was selected for fixing screw. Effective depth was also calculated not to be destroyed because of high pressure generated during engine cycle. Fig.2.12 shows picture image of screw. Formula is following.

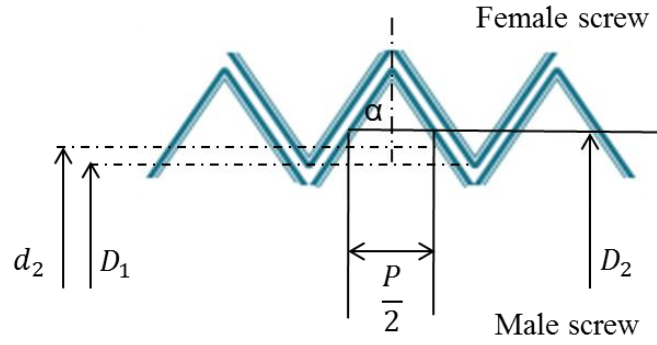


Figure 2.12. Picture Image of Screw

$$\tau_a = \frac{W}{A}$$

$$\Leftrightarrow z = \frac{3 \cdot p \cdot b l_{hole}}{\pi D_1 \tau_a \{P/2 + (d_2 - D_1 \tan \alpha)\}}$$

$$L_{screw} = P(z + 0.5) \cong 0.2$$

W	: Load
A	: Area
z	: The number of thread ridges
p	: Pressure
b	: Width of hole for plasma observation
l_{hole}	: length of hole for plasma observation
D_1	: Inside diameter of the screw
τ_a	: Shear stress of aluminum screw
P	: Pitch
d_2	: Effective diameter
α	: Angle of screw
L_{screw}	: Screw length

Screw length has to be bigger than the value of L to withstand high pressure inside the thruster. Therefore, screw length of M3 is 3 mm. This part does not have the mechanism like inner moat due to too high manufacturing cost. Acrylic window is attached from outside to this part.

Moreover, new tube was designed in order to the thruster without reed valve. New tube becomes the thruster without reed valve to be connected with the tube of the thruster with reed valve (Fig.2.11.). The tube has about 300 mm length, the thickness 0.8mm, and acrylic window for plasma propagation. The picture of the thruster without reed valve and the thruster with reed valve are shown at the end of this chapter.

2.3 Design of Reed Valve

As described above, reed valve which can open widely and to be free from plastic deformation is needed. In past study, SUS304CSP is selected as the material of reed valve. However, plastic deformation was occurred when reed valve has the 0.2 mm thickness was used. Although plastic deformation does not be occurred by increasing the thickness of reed valve, the thickness has four-orders to the displacement of reed valve. Increasing the thickness relates to decrease of refilling enormously. For example, plastic deformation does not occurred when reed valve (material: SUS304CSP) which has the thickness 0.3 mm is used. But maximum displacement of the reed valve is about 4 mm. When reed valve which has the thickness 0.2 mm is used, average displacement is over 7 mm contrastively. Therefore, the material of reed valve is selected. In past study, carbon-fiber-reinforced plastic (CFRP) has higher performance to the refilling than SUS304CSP as the material of reed valve. However, there are 3 problems in case of using CFRP.

1. CFRP does not have clear yield stress
2. Reed valve of CFRP would be destroyed in the experiment due to brittle material
3. CFRP does not have resistance to heat

The most important point is 1. It is difficult to design reed valve due to this reason. Therefore, titanium (Ti) is considered as the material. Table 2.1 shows mechanical property of SUS304CSP, CFRP and Ti.

Table.2.1. Mechanical Property of SUS304CSP, CFRP and Ti

	Density $\left(\frac{g}{cm^3}\right)$	Yield stress $\left(\frac{N}{mm^2}\right)$
SUS304CSP	7.7~7.9	255
CFRP	1.5	-
Ti	4.4	920

From Table.2.1, Ti has lightness, high yield stress and resistance to heat. Because of this, Ti is selected as the material.

Next, increasing the length of hole for reed valve was considered in order to increase refilling volume. First of all, average negative pressure generated during engine cycle was estimated by using past experimental result. The displacement of reed valve depends on negative pressure. Moreover, the cantilever was considered as calculation model. Fig.2.13 shows the model. Calculation formula is also following. From this, average negative pressure 0.5 MPa was estimated.

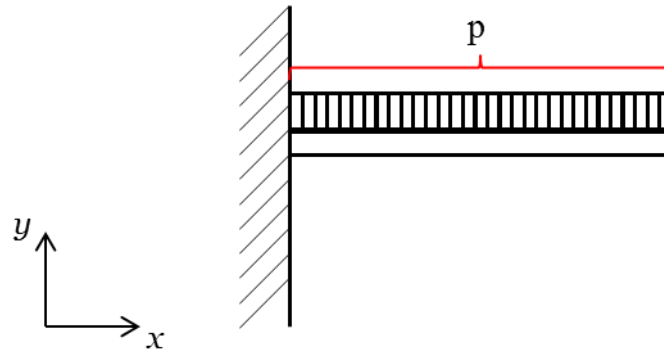


Figure 2.13. Proximate Model of Intensity Calculation

$$y_{MAX} = \frac{\Delta p L^4}{8EI_z}$$

$$M_{MAX} = \frac{p \cdot b \cdot L^2}{2}$$

$$\sigma_{MAX} = \frac{M_{MAX}}{b \cdot t^2/6}$$

y_{MAX}	: Maximum displacement
Δp	: Negative pressure
L	: Length of reed valve
E	: Young's modulus of Ti
I_z	: Second moment of area
M_{MAX}	: Maximum moment
b	: Width o reed valve
σ_{MAX}	: Maximum stress
t	: Thickness of reed valve

The moment reed valve opens, the length of hole is important for the displacement. Because of this, that length was estimated by using above formula. Fig.2.14 shows relationship between stress at the fixed end of reed valve and length of hole. From this result, it was decided length is 23 mm for the hole.

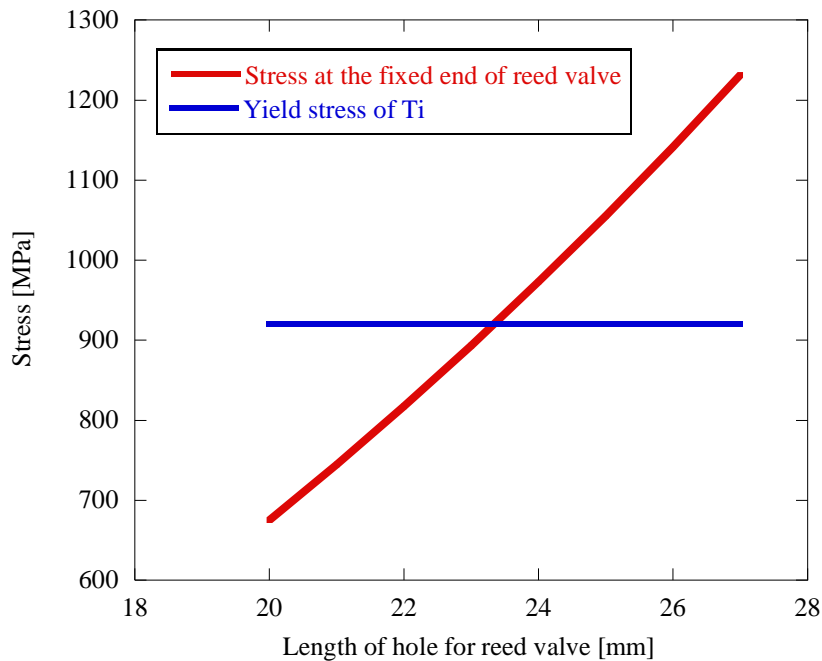


Figure 2.14. Relationship between Stress and Length of Hole for Reed Valve

Moreover, shape of reed valve was also considered to increase the displacement under allowable stress. Allowable stress is about 707 when factor of safety is 1.3. Table 2.2 and 2.3 show stress and the displacement of taper reed valve respectively. Table.2.2 is in the case of the width-taper and Table.2.3 is in the case of the thickness and width-taper. First, optimum width was decided from Table.2.2. It is from 14 mm to 12 mm and from 16 mm to 12 mm. Next, final shape of reed valve was decided by changing the thickness in case of width which is from 14 mm to 12 mm and width which is from 16 mm to 12 mm. By computer aided design (CAD) analysis, final shape is width of 16 mm-12 mm and thickness of 0.35 mm-0.15 mm. Fig.2.15 and Fig.2.16 shows picture image of computer aided design (CAD) analysis. The displacement and the stress are shown by separating the color. Maximum stress and the displacement are shown in red color.

Finally, natural frequency of Ti-taper reed valve was measured by CAD and experiment. Fig.2.17 shows picture image of that experiment. Natural frequency of Ti-taper reed valve has to be over

frequency of pressure oscillation inside the thruster. If natural frequency is lower, reed valve could not open appropriately to adjust pressure oscillation. From that experiment, natural frequency of Ti-taper reed valve was 470 Hz. Here, frequency of pressure oscillation in past experiment was used. Fig.2.18 shows its pressure oscillation at closed end. From that graph, frequency of pressure oscillation is about 200 Hz. Natural frequency of reed valve is over that of pressure oscillation. Hence, this reed valve can be used to the thruster.

Table2.2 Stress and Displacement (Thickness: 0.4-0.2)

Width (mm)	14-10	14-12	16-10	16-12
Stress (MPa)	511	556	480	519
Displacement (mm)	5.07	5.43	4.81	5.15

Table2.3 Stress and Displacement

Thickness (mm)	0.35-0.2	0.35-0.15	0.35-0.2	0.35-0.15
Width (mm)	14-12	14-12	16-12	16-12
Stress (MPa)	556	722	672	679
Displacement (mm)	5.43	8.72	7.15	8.28

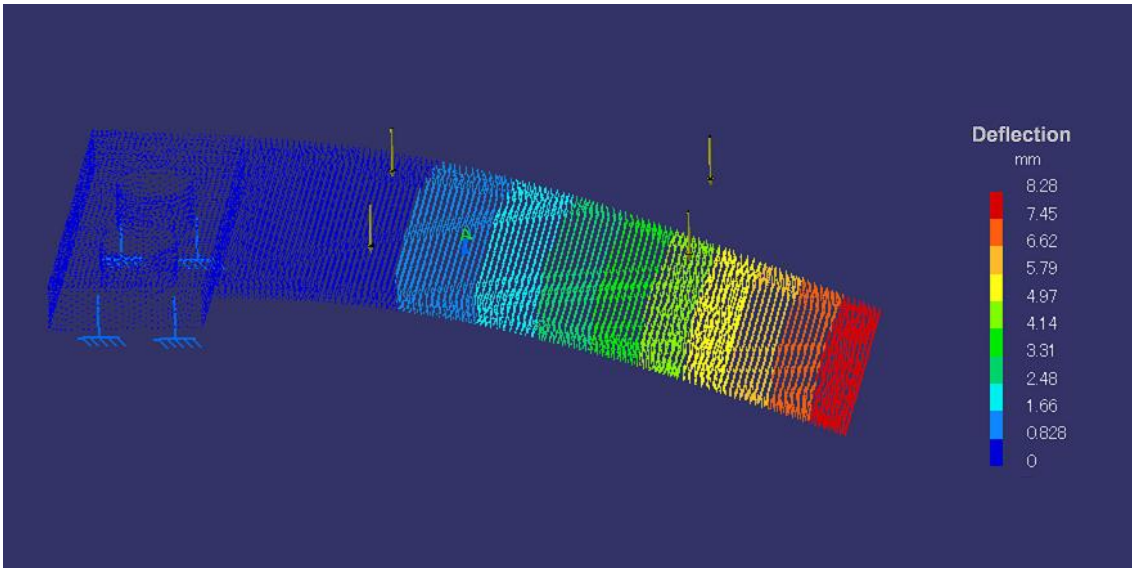


Figure 2.15. Picture Image of Displacement Analysis

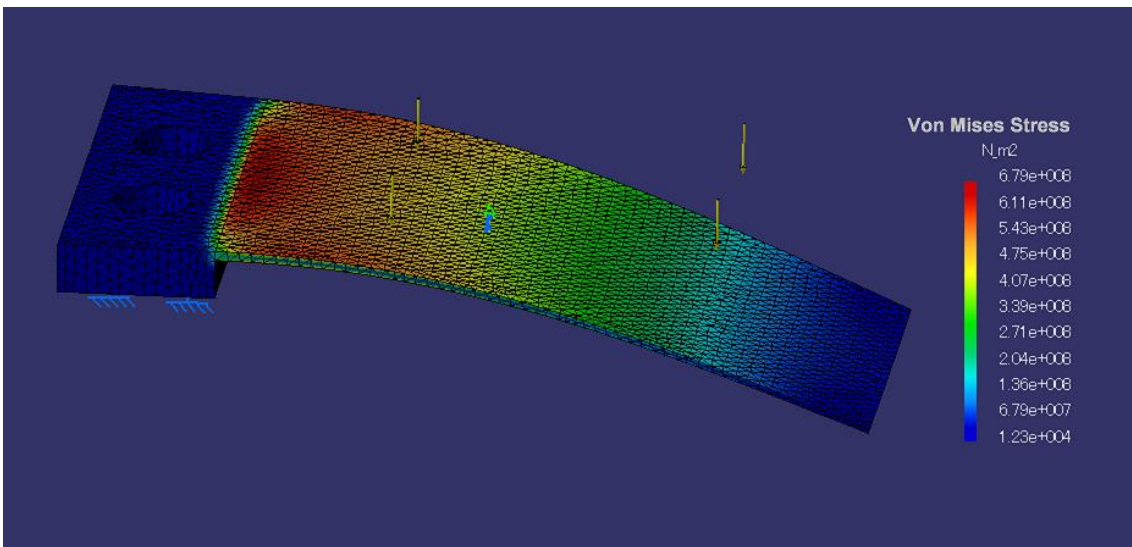


Figure 2.16. Picture Image of Stress Analysis

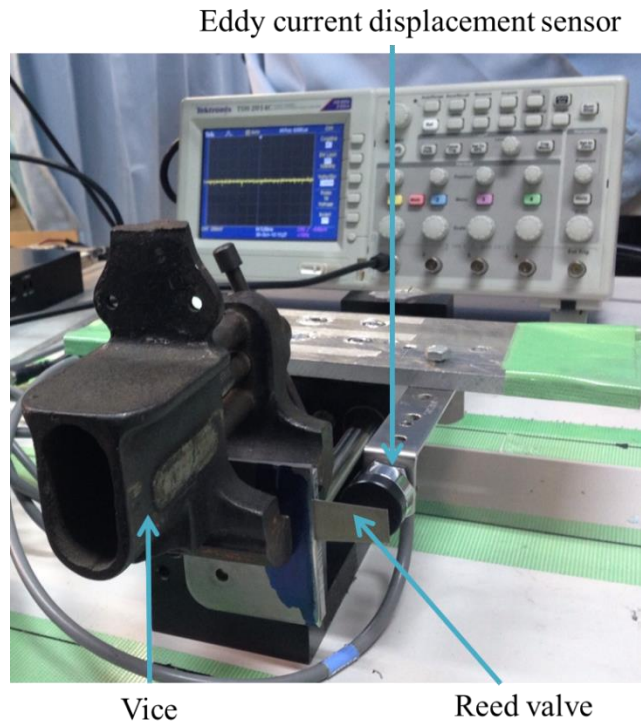


Figure 2.17. Picture Image of the Experiment for Measurement of Natural Frequency

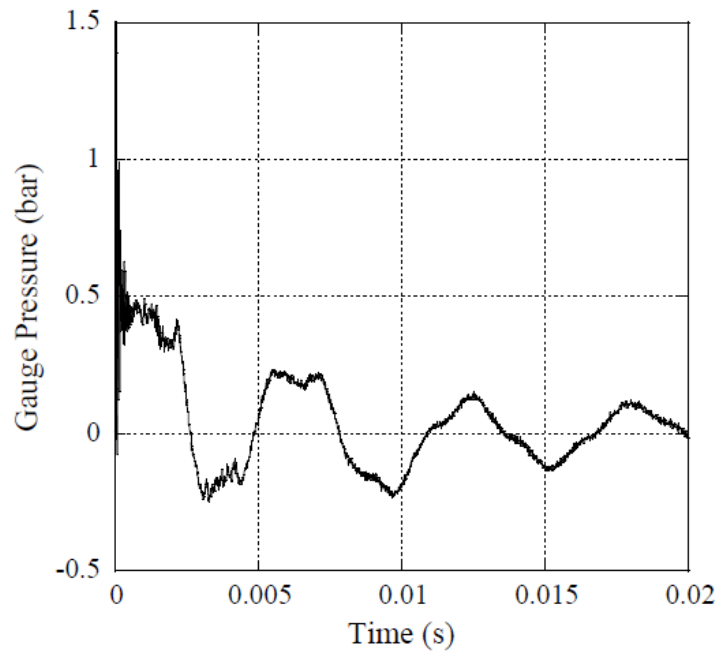


Figure 2.18. Pressure oscillation at Closed End. Reprinted from [15]

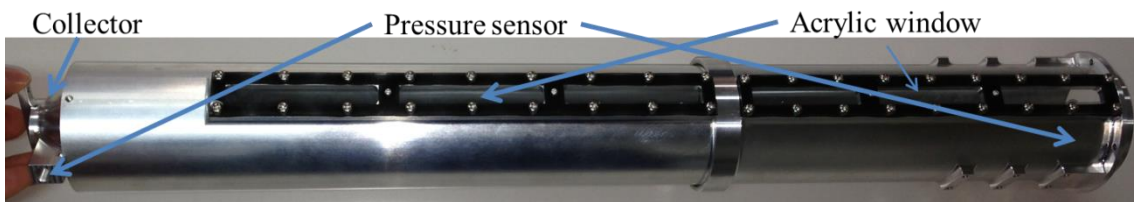


Figure 2.19. Thruster without Reed Valve

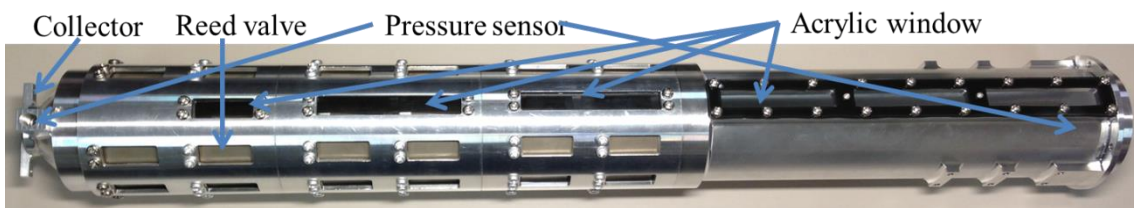


Figure 2.20. Thruster with Six-Stage Reed Valve

Chapter 3

Effect of Ti-Taper Reed Valve and Thrust Performance

3.1 Thrust Parameter of Microwave Rocket

In past study, impulse of Microwave Rocket was measured in various conditions. Oda et al conducted the experiment by changing input peak power of microwave beam P_{peak} and pulse duration time τ individually. In this experiment, it was found that rate of impulse increment in case of high power condition was decreased in comparison to low power condition. It means that momentum coupling coefficient C_m was saturated in case of high power condition [16]. Likewise, the rate of impulse increment in case of long pulse duration time was decreased [17]. From this experiment, it can be said that momentum coupling coefficient C_m are expressed as following equation.

$$C_m = \frac{I}{P_{peak} \cdot \tau}$$

C_m	: Momentum coupling coefficient
I	: Impulse
P_{peak}	: Input peak power of microwave beam
τ	: Pulse duration time

C_m was decreased when plasma propagates over the open end of the thruster. In short, there is optimum plasma length generated in an engine cycle. Fig.3.1 shows relationship between C_m and pulse duration time. Normalized plasma length was defined as following equation.

$$l = \frac{U_{\text{ioniz}} \cdot \tau}{L}$$

l	: Normalized plasma length
U_{ioniz}	: Propagation velocity of ionization front
τ	: Pulse duration time
L	: Thruster length

If plasma propagates at the open end of the thruster, this normalized plasma length is unity. As shown in fig.3.1, optimum plasma length exists between 0.6 and 0.8. Besides, U_{ioniz} is decided by input peak power of microwave beam P_{peak} . However, it was difficult to decide optimum plasma length.

Furthermore, thrust was measured by changing repetitive pulse frequency under air flow condition. The result was that the thrust was increased linearly under low power condition [18].

Up here, it is clarified that there are four parameters which decides the thrust. In summary, the thrust F is defined as following equation.

$$F = P_{\text{peak}} \cdot \tau \cdot f \cdot C_m$$

F	: Thrust
P_{peak}	: Input peak power of microwave beam
τ	: Pulse duration time
f	: Repetitive pulse frequency
C_m	: Momentum coupling coefficient

Here, product of τ and f is called duty cycle ϕ . If continuous wave was irradiated, ϕ is unity. However, Oda et al conducted the measurement of impulse under repetitive pulse frequency. Fig.3.2 shows impulse-bit decrement under multi-pulse operation. As shown in fig.3.2, C_m was decreased drastically after second pulse without air-flow. C_m was also decreased in case of air-flow [19]. Hence, C_m is decreased under multi pulse operation.

From past study, it is important to prevent C_m decrement by reed valve air-breathing system for increasing time-averaged thrust. Moreover, repetitive pulse frequency is less than 100 Hz due to avoid anomalous ignition. Anomalous ignition is mentioned hereinafter.

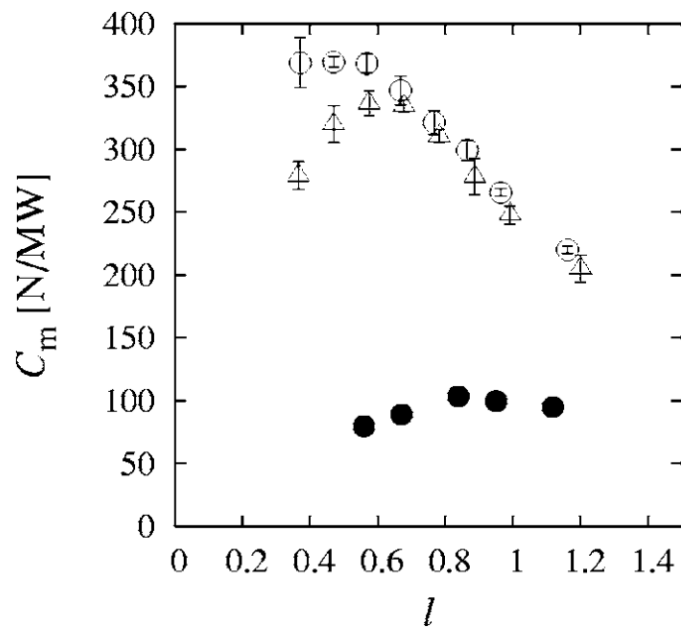


Figure 3.1. Relationship between C_m and normalized plasma length l . Reprinted from [14]

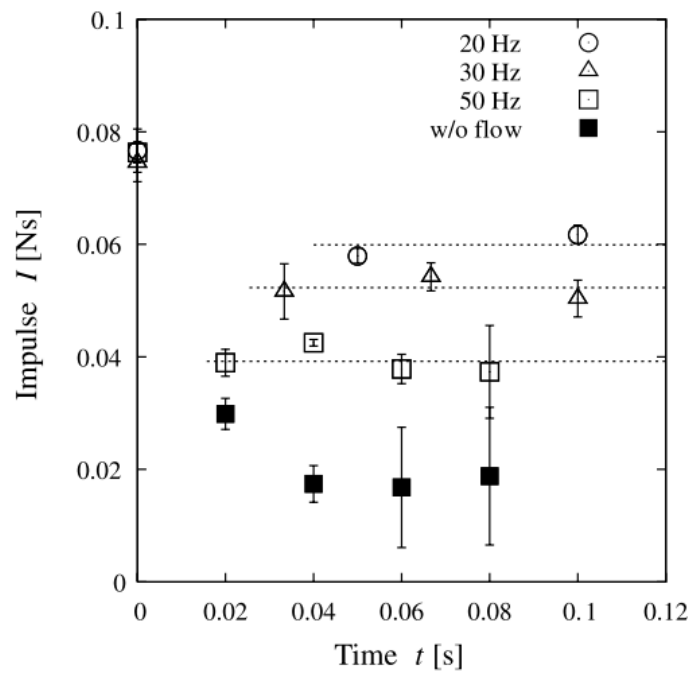


Figure 3.2. Impulse-Bit Decrement under Multi-Pulse Operation. Reprinted from [16]

3.2 Objective of This Experiment

When reed valve of thickness 0.2 mm was used, impulse was decreased due to plastic deformation. When reed valve of thickness 0.3 mm was used, plastic deformation did not be occurred. Refilling volume, however, was decreased. Furthermore, as mentioned above, it was found that the decrement of plateau pressure was prevented by attaching reed valve to the thruster. Refilling volume has to be increased much further in order to validate reed valve air-breathing system.

Therefore, two objectives were decided.

1. To verify refilling performance of Ti-taper reed valve by comparing SUS304CSP reed valve and propagation velocity of shock wave with or without reed valve.
2. To increase the thrust by attaching Ti-taper reed valve to the thruster when duty cycle is changed.

We have already known that effect of increasing the refilling volume is found as the effect of preventing the thrust decrement. If there is the effect of preventing the thrust decrement, time-averaged thrust is increased at same duty cycle. Furthermore, as mentioned above, anomalous ignition was occurred due to remain of electrons inside the thruster when repetitive pulse frequency was over 100 Hz in past experiment. Hence, high pulse duration time and low repetitive pulse frequency is operated to prevent anomalous ignition in this experiment.

3.3 Experimental Apparatus

3.3.1 Experimental System

In this study, the experiment was conducted by using transmit mirror to prevent microwave spread and taper to collect microwave from transmit mirror. Vertical launch system was assumed in this system. Fig.3.3 shows conceptual schematic of this system and Fig.3.4, Fig.3.5 shows picture image of this system. Alignment was conducted by using thermal paper, infrared camera (IR camera) and high speed camera.

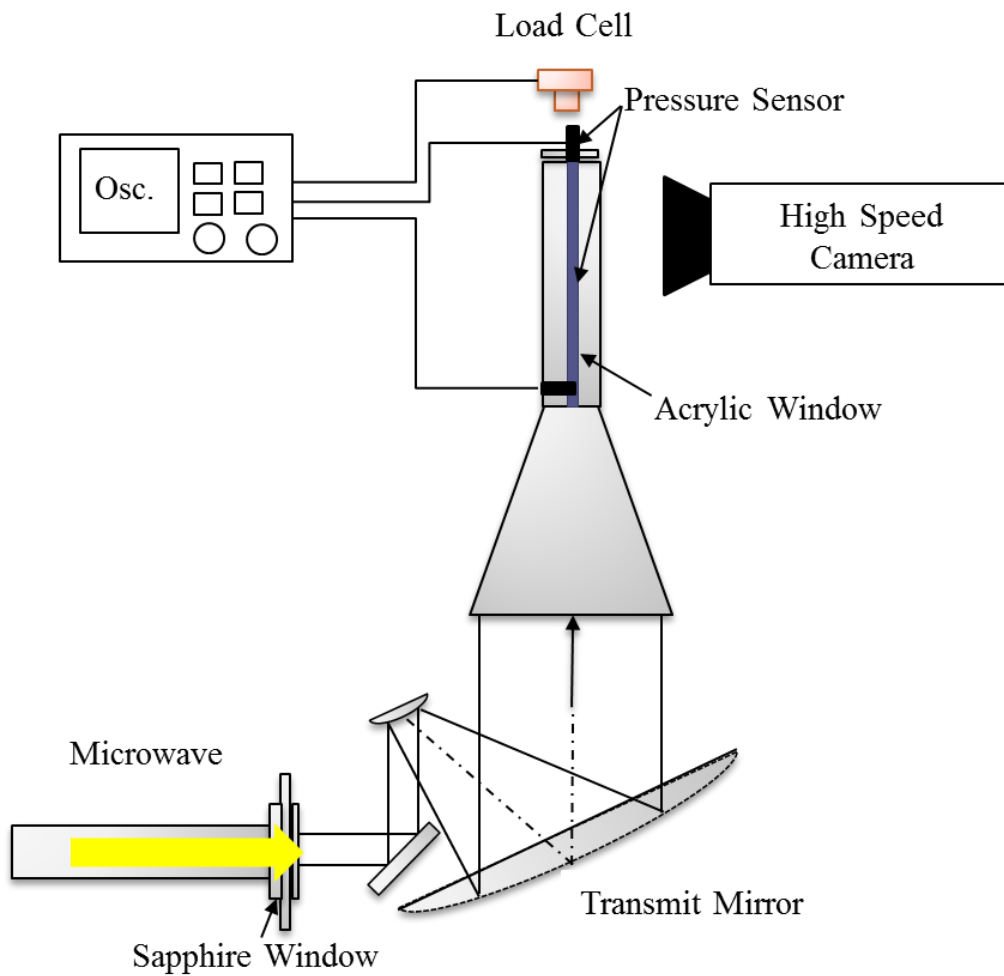


Figure 3.3. Conceptual Schematic of Experimental System

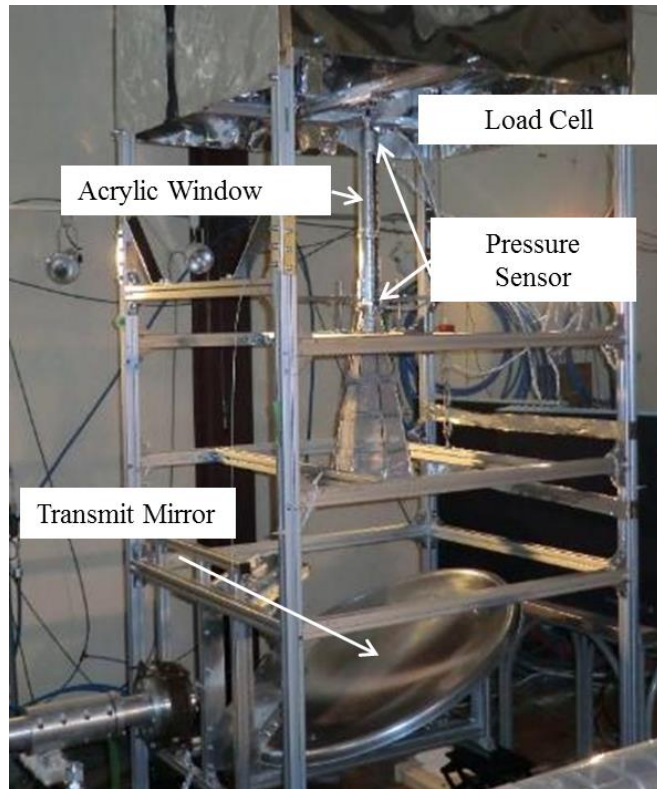


Figure 3.4. Picture Image of Experimental Setup



Figure 3.5. Picture Image of Experimental Setup

Furthermore, three thrusters and ti-taper reed valve were used in this experiment. Fig.3.6, Fig.3.7 and Fig.3.8 show picture image of these thruster. These are thruster without reed valve, thruster with two-stage reed valve and thruster with six-stage reed valve. Fig.3.9 shows the detail of Ti-taper reed valve. Because anomalous ignition was occurred as described hereinafter, the thruster with two-stage reed valve was used. The attachment for increasing the thruster length was used in the thruster with two-stage reed valve. It has screw mechanism on the top and bottom, inside diameter of 56 mm and the thickness of 0.8 mm. Besides, its material is A5056. The thruster with two-stage reed valve has 16 reed valves and the thruster with six-stage reed valve has 48 reed valves. Moreover, all thrusters have common collector and pressure sensor can be used at the top and bottom of the thruster.

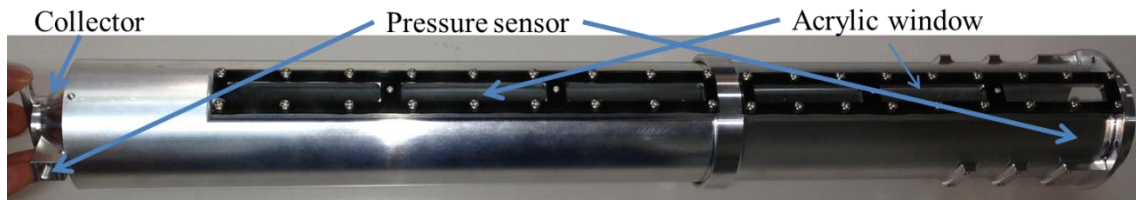


Figure 3.6. Thruster without Reed Valve

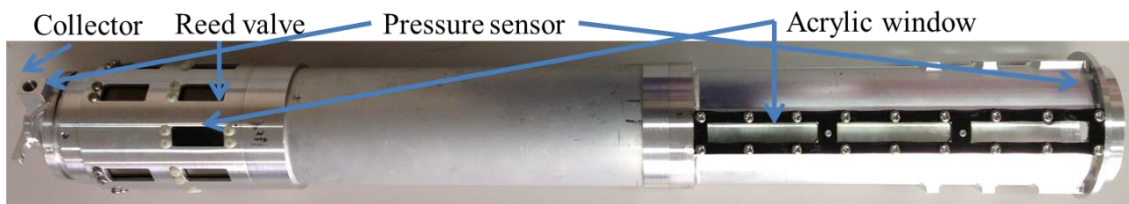


Figure 3.7 Thruster with Two-Stage Reed Valve

The Number of Reed Valve : 16

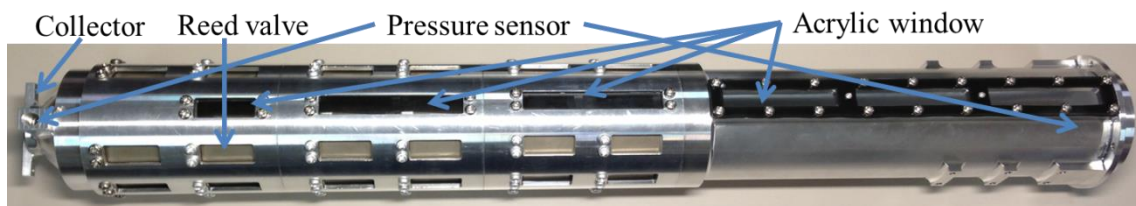


Figure 3.8 Thruster without Six-Stage Reed Valve

The Number of Reed Valve : 48



Width	: From 16 mm to 12 mm
Thickness	: From 0.35 mm to 0.15 mm
Material	: Titanium
Natural Frequency	: 470 Hz

Figure 3.9. Picture Image of Taper-Titanium Reed Valve

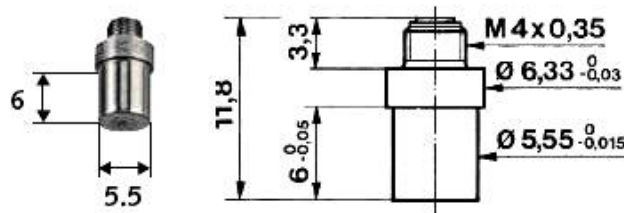
3.3.2 Measurement System

Measure system is shown from Fig.3.10 to Fig.3.14. Load cell was used for measurement of the thrust. The thrust was estimated from impulse which integrated the value of load cell. Pressure sensor was used for confirming pressure history, abnormal pressure wave due to anomalous ignition and propagation velocity of shockwave. Eddy current displacement sensor was used in order to measure the displacement of reed valve. The fixture was manufactured to be able to measure the displacement of reed valve in vertical launch system. Finally, propagation velocity of ionization front and anomalous ignition were confirmed by using high speed camera and home movie camera.



Model	: KYOWA Electronics LM-10KA-P
Resonant frequency	: 21 kHz
Rated capacity	: 100 N

Figure 3.10. Picture image of load cell



Measurement system	: 0~200 bar
Natural frequency	: 400 Hz
Operating temperature	: -196~200°C
Crashworthy	: 10000 G
Mass	: 1.7 g

Figure 3.11. Picture Image of Pressure Sensor



Model	: NAC MEMRECAM HX-3
Pixel	: 2560 × 1920
Shutter speed	: 1,300,000 Hz

Figure 3.12. Picture Image of High Speed Camera



Model	: KEYENCE EX-422V
Measurement range	: 0~10 mm
Sampling frequency	: 40000 Hz
Response time	: 0.075 ms
Mass (sensor head)	: About 200 g
Mass (amplifier unit)	: About 235 g

Figure 3.13. Picture Image of Eddy Current Displacement Sensor

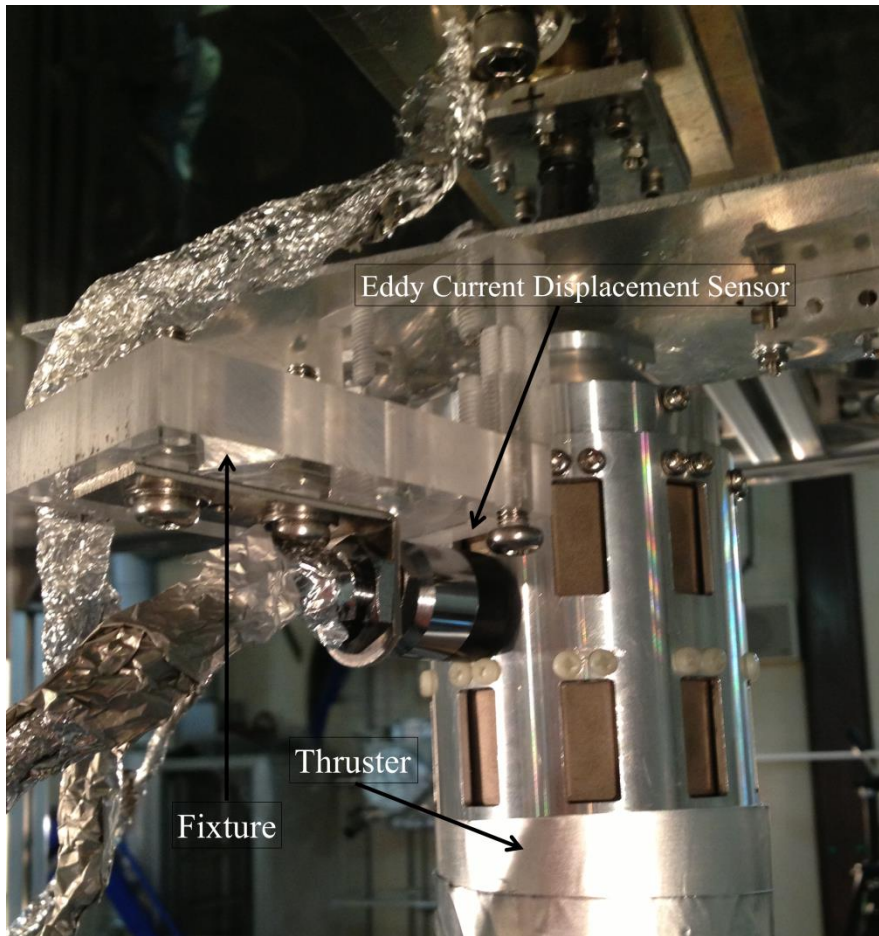


Figure 3.14. Picture Image of Fixture for Eddy Current Displacement Sensor

3.4 Result of Experiment

3.4.1 Effect of Reed Valve

Figure 3.15 shows displacement of Ti-taper reed valve. As shown in Fig.3.16, the displacement of Ti-taper reed valve was 8 mm. In this experiment, this reed valve opened from 4mm to 11 mm according to pressure oscillation inside the thruster in case of generating the thrust. When the thrust did not be generated, the displacement of this reed valve was quite small. Moreover, Fig.3.16 shows Ti-taper reed valve after experiment. It was found that plastic deformation did not be occurred from this picture image.

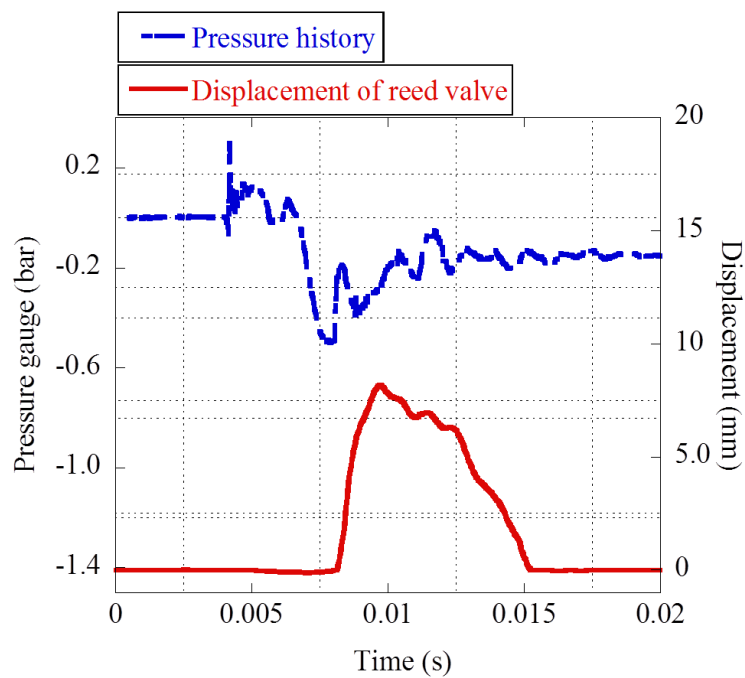


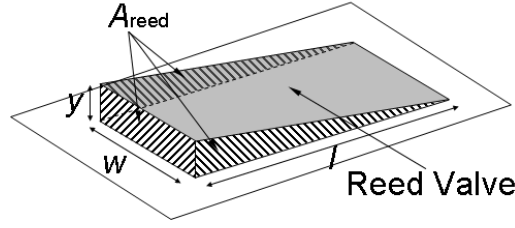
Figure 3.15. Displacement of Reed Valve (Ti-Taper Reed Valve)



Figure 3.16. Reed Valve after the Experiment

Moreover, partial filling rate (value divided refilling volume by total volume inside the thruster) was compared in case of 0.2 mm SUS304CSP and Ti-taper reed valve. First of all, Fig.3.17 shows conceptual schematic of refilling area. When reed valve opens, fresh air get through inside the thruster from three areas. Partial filling rate was calculated by time integral of the displacement by using mass flow equation. That equation is following [20]. Besides, partial filling rate shows Table 3.1. It was already found that when partial filling rate is increased, the thrust decrement is prevented. As shown in Table.3.1, partial filling rate of Ti-taper reed valve is about 1.7 higher than that of SUS304CSP reed valve.

From these results, it can be said that Ti-taper reed valve has higher refilling performance and intensity on load than SUS304CSP reed valve.



y: Displacement, w: width, l: length, A_{reed} : Refilling area

Figure 3.17. Conceptual Schematic of Refilling Area

$$\dot{m} = \rho u A_{reed}$$

$$\therefore \dot{m} = \rho_0 \left(\frac{p}{p_0} \right)^{\frac{1}{\gamma}} \cdot \sqrt{\frac{2\gamma}{\gamma-1} \frac{p_0}{\rho_0} \left[1 - \left(\frac{p}{p_0} \right)^{\frac{\gamma-1}{\gamma}} \right]} \cdot A_{reed}$$

\dot{m}	: Mass flow
ρ	: Density
u	: Velocity
A_{reed}	: Opening area of reed valve
ρ_0	: Density in atmospheric pressure
p	: Pressure
p_0	: Atmospheric pressure
γ	: Ratio of specific heat

Table3.1. Partial Filling Rate

	Partial Filling Rate
SUS304CSP reed valve (Fig.2.5)	0.19
Ti-taper reed valve (Fig.3.10)	0.32

As mentioned Fig.2.2, impulse is obtained by the product of plateau pressure, plateau pressure time and area of closed end. Plateau pressure time is sum of the time which propagation velocity of shockwave propagates from closed end to open end and the time which expansion wave propagates from open end to closed end. Because Mach number of expansion wave is unity at all time, the time which expansion wave propagates from open end to closed end is same. Therefore, the velocity of shockwave should be slow to increase plateau pressure time. Increasing plateau pressure time relates to increasing the impulse.

It is expected to decrease the increment of propagation velocity of shockwave by using the thruster with reed valve because there is cooling effect inside the thruster by reed valve. Therefore, the propagation velocity of shockwave was compared in case of the thruster without reed valve and the thruster with two-stage reed valve. Fig.3.18 shows the propagation velocity of shockwave each pulse compared to with or without reed valve.

From this figure, the propagation velocity of shockwave is increased in both cases as pulse count is increased. The reason why the propagation velocity of shockwave is increased is that inside temperature is also increased as pulse count is increased. Besides, the rate of velocity increase was prevented by using the thruster with two-stage reed valve. At fifth time of pulse count, the propagation velocity of shockwave in case of the thruster with reed valve was 0.8 lower than that without reed valve. Hence, it was found that there was the effect of decreasing the propagation velocity of shockwave. In short, it can be said that plateau pressure time is increased and the thrust is also increased by attaching the reed valve to the thruster.

However, as described hereinafter, when anomalous ignition is occurred, high pressure is not generated at the top of the thruster normally and the displacement of reed valve is decreased. Besides, there is no cooling effect. Because of this, it is important to prevent anomalous ignition for cooling effect.

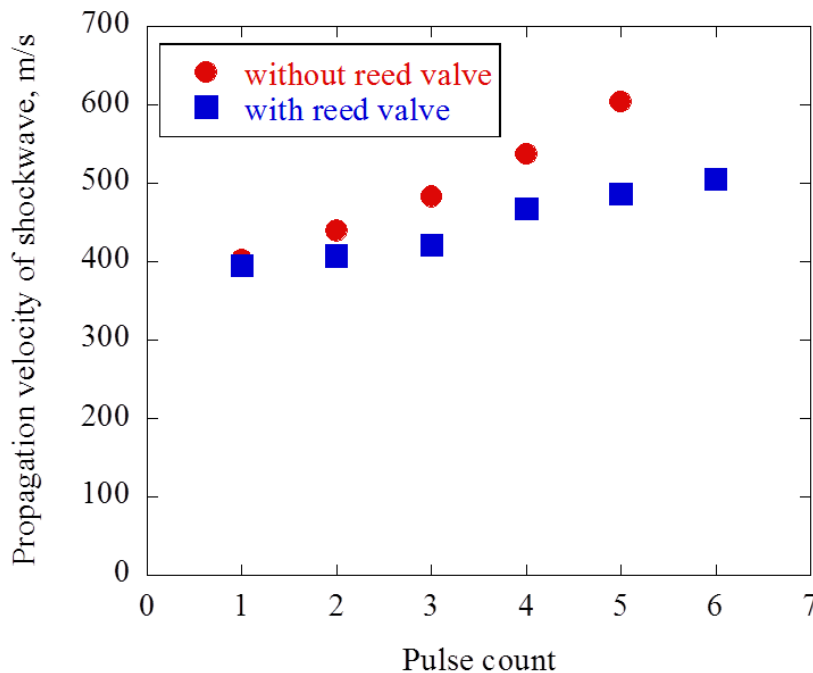


Figure 3.18. Relationship between Propagation Velocity of Shockwave and Pulse Count

3.4.2 Relationship between Thrust and Duty Cycle

Figure 3.19 shows relationship between the thrust and duty cycle when the thruster without reed valve is used. Pulse duration time was also shown at upper right in Fig.3.19. From this figure, it was found that the thrust was increased until around 15 % duty cycle. Because refilling time was enough in low duty cycle, plasma propagated until at the bottom of the thruster. Therefore, C_m did not be decreased. Furthermore, C_m was able to be estimated from gradient of Fig.3.19 because power of microwave was constant in this experiment. C_m was about 22 in this case. As just described, C_m is too small to launch vertically.

One of the reasons that the thrust was decreased over 15 % duty cycle was that refilling time was decreased when that area was operated. The decrement of refilling time related to increasing the volume of hot and expansive gas inside the thruster. Therefore, C_m was decreased because the condition inside the thruster was different from the condition of first pulse. The tendency was seen over 70 Hz especially. Moreover, it was also found that repetitive pulse frequency was limited until about 150 Hz in case of this thruster because pressure oscillation continued until that frequency. Therefore, refilling time is decreased over about 150 Hz. Fig.3.20 shows limit of repetitive pulse frequency.

The other is that anomalous ignition was occurred inside the thruster. As mentioned above, we have already known optimum plasma length. However when anomalous ignition was occurred, it is impossible to adjust the optimum plasma length. There is the process which the thrust does not be generated due to anomalous ignition. First, that phenomenon occurs along the way of the thruster. When it happens, the plasma which is maintained inside the thruster becomes short and plateau pressure time was decreased. Moreover, C_m was decreased when plasma propagates outside the thruster. Therefore, the thrust was decreased gradually. Fig.3.21 shows anomalous ignition along the way of the thruster. This photo is printed frame-by-frame with the constant interval time. The reason why anomalous ignition is occurred is that electronic density is increased inside the thruster in high repetitive pulse frequency between pulse and pulse. Besides, there are a lot of edges inside the thruster. The concentration of electric field is generated in that point and the ignition is occurred. The thrust was decreased gradually in this phase.

After anomalous ignition along the way of the thruster, anomalous ignition was finally occurred only at the bottom of the thruster. The thrust cannot be generated when it happens. Fig.3.22 shows anomalous ignition at the bottom of the thruster.

From past study and this experiment, anomalous ignition is the biggest reason of thrust decrement. Therefore, it is the most important to solve this phenomena for Microwave Rocket.

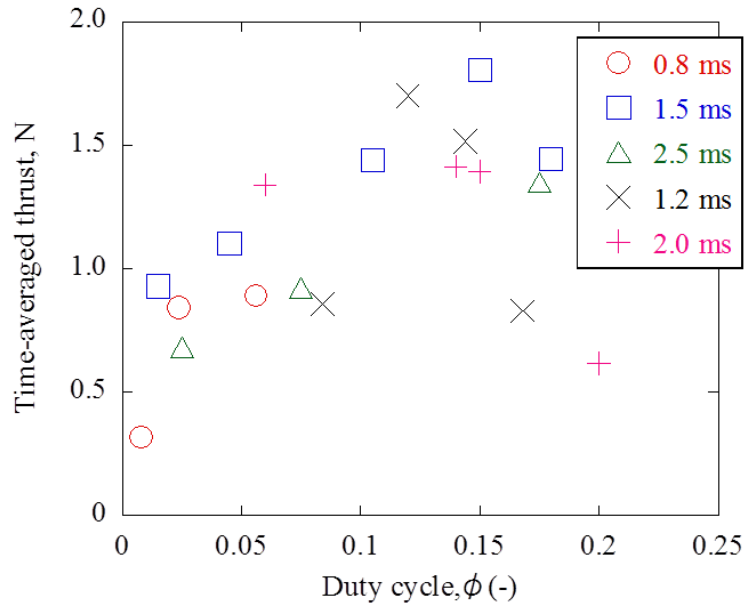


Figure 3.19. Relationship between Thrust and Duty Cycle (Thruster without Reed Valve)

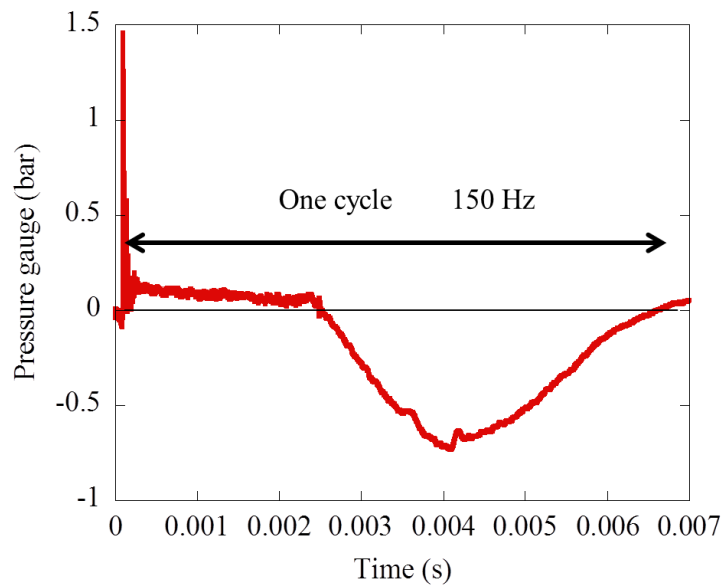


Figure 3.20. Limit of Repetitive Pulse Frequency

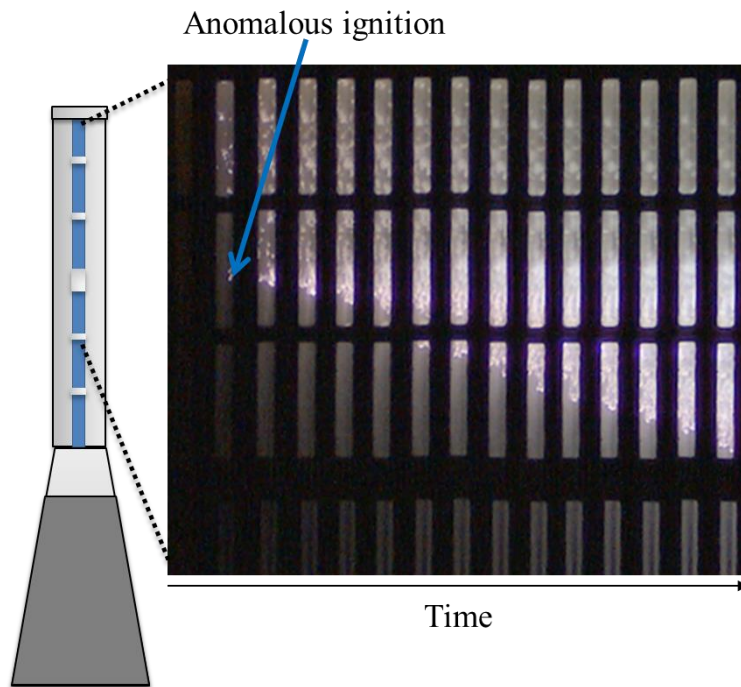


Figure 3.21. Anomalous Ignition along the Way of the Thruster
 (This frame was taken frame-by-frame with the constant time interval)

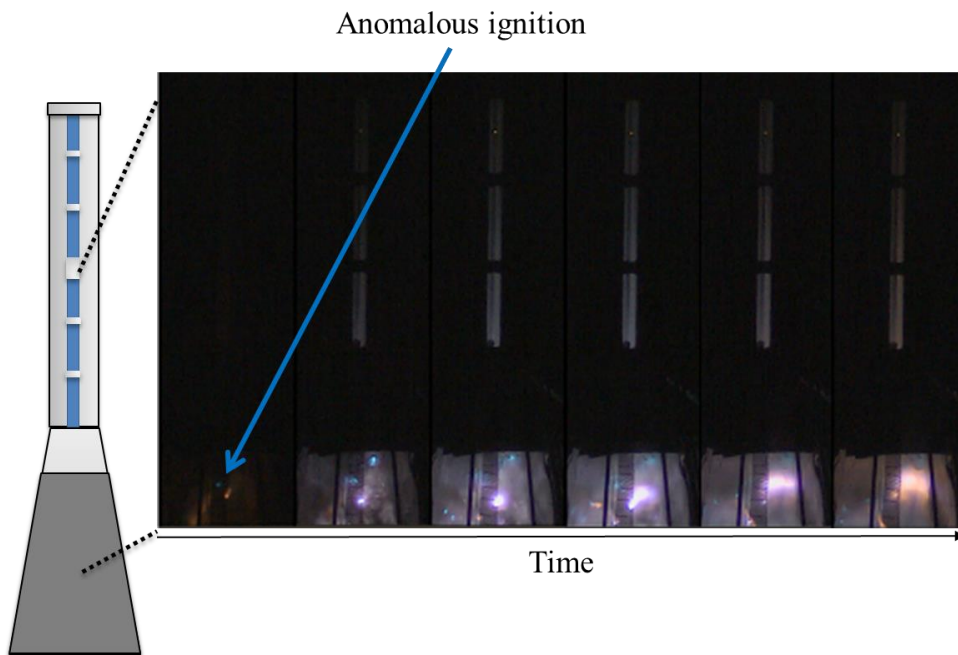


Figure 3.22. Anomalous Ignition at the Bottom of the Thruster
 (This frame was taken frame-by-frame with the constant time interval)

Figure 3.23 shows relationship between the thrust and duty cycle when the thruster with two-stage reed valve is used. Pulse duration time was also shown at upper right in Fig.3.23. As shown in Fig.3.23, the thrust was increased until around 10 % duty cycle. Moreover, its thrust was about same in comparison to the thrust without reed valve. C_m was estimated similarly and it was about 34. Compared to C_m in case of the thruster without reed valve, C_m was about 1.6 larger under 10 % duty cycle areas.

The reason why the thrust was decreased over around 10 % duty cycle was anomalous ignition was generated at the around reed valve in high repetitive pulse frequency and pulse duration time. Therefore, plasma which can be maintained was short with respect to each pulse count and C_m was decreased gradually. Besides, it was easy to remain electronic density at the bottom of the thruster and anomalous ignition was occurred finally. The same thrust, however, was generated in small duty cycle compared to the result of the thruster without reed valve. In short, the thrust decrease was prevented by attaching the reed valve to the thruster. If anomalous ignition does not occurred by changing the mechanism of the thruster (for example, to attach the electrical insulation part to the thruster or to insert the mesh which can reflect the microwave), it is possible to increase duty cycle and the thrust eventually.

Fig.3.24 shows relationship between the thrust and duty cycle using the thruster with six-stage reed valve. Pulse duration time was also shown at upper right in Fig.3.24. As shown in Fig.3.24, the thrust was small compared with the result of the thruster with two-stage reed valve. The thrust tendency, however, was same to the result of the thruster with two-stage reed valve. The reason of small thrust was that anomalous ignition was occurred at the connecting part of the thruster with reed valve and the tube and plasma which was able to be maintained was too short to generate the thrust. Moreover, pressure wave propagates both directions. Besides, the displacement of reed valve was small due not to generating high pressure at the top of the thruster.

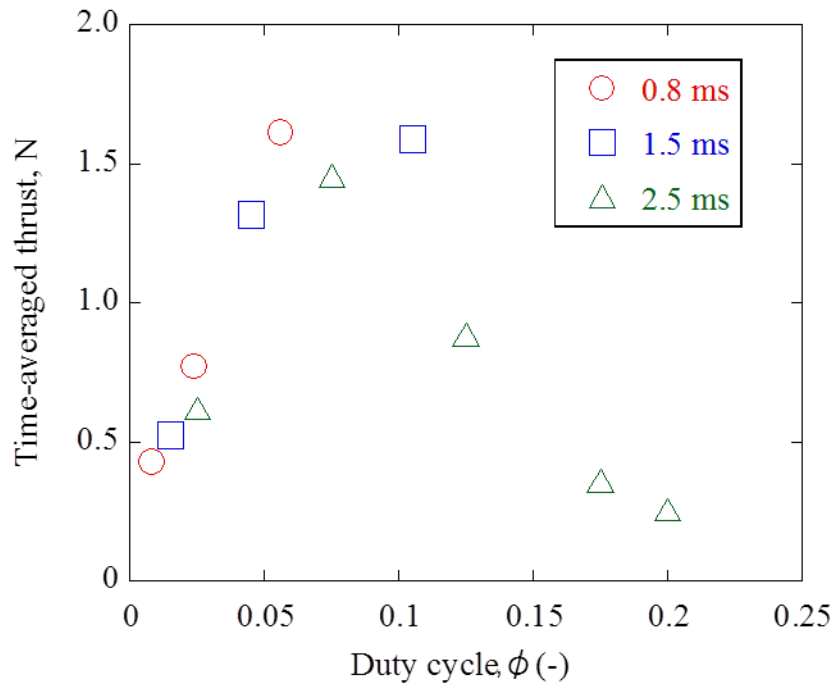


Figure 3.23. Relationship between Thrust and Duty Cycle
(Thruster with Two-Stage Reed Valve)

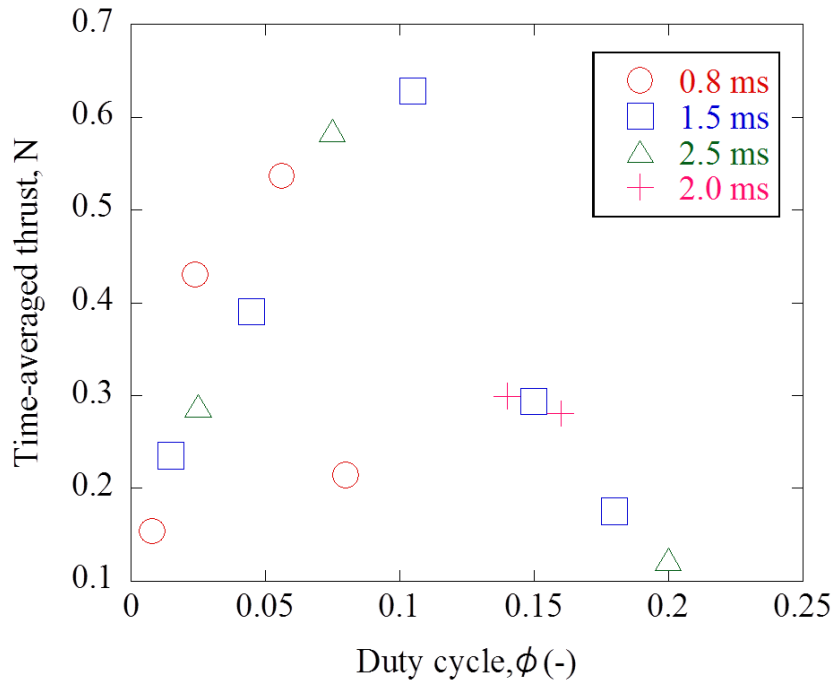


Figure 3.24. Relationship between Thrust and Duty Cycle
(Thruster with Six-Stage Reed Valve)

Figure 3.25 shows picture image of anomalous ignition when the thruster with six-stage reed valve was used. Main reason of anomalous ignition when the thruster with six-stage reed valve was used is misalignment and the existence of reed valve and acrylic window attachment (Fig.2.7.). Fig.3.26 shows picture image of internal thruster. It was conceivable that microwave beam was irradiated at this part and the ignition started. Therefore, reed valve and acrylic window attachment was replaced from metal to insulator. Fig.3.27 shows reed valve and acrylic window attachment of metal. Its material is aluminum. Fig. 3.28 shows reed valve and acrylic window attachment of insulator. These materials are acryl and plastic. Here, Fig.3.29 and Fig.3.30 shows pressure history at the top of the thruster in case of metal attachment and insulator attachment respectively. Besides, the thruster with six-stage reed valve is used in fig.3.29 and the thruster with two-stage reed valve is used in Fig.3.30. Although the number of reed valves is different, high pressure was generated at the top of the thruster by replacing from metal to insulator attachment. Because of this, the material of an edge inside the thruster like reed valve and acrylic window attachment should be insulator in future thruster.

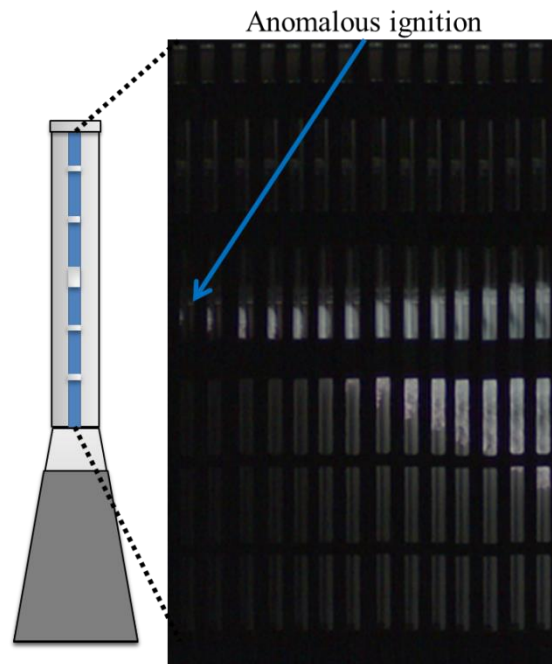
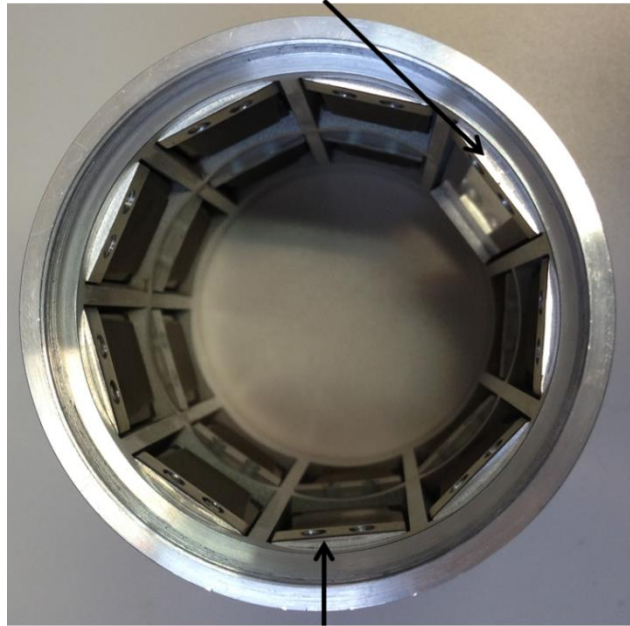


Figure 3.25. Anomalous Ignition (Thruster with Six-Stage Reed Valve)
 (This frame was taken frame-by-frame with the constant time interval)

Bulge of attachment of acrylic window



Bulge of attachment of reed valve

Figure 3.26. Cross-Section View of the Thruster with Reed Valve



Figure 3.27. Reed Valve and Acrylic Window Attachment of Metal



Figure 3.28. Reed Valve and Acrylic Window Attachment of Insulator

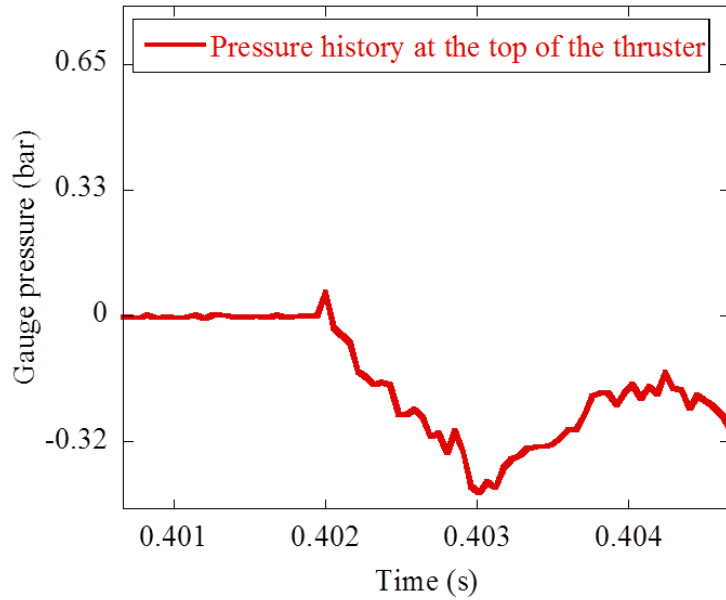


Figure 3.29. Pressure History in Case of Metal Attachment (Pulse Count: Fifth)

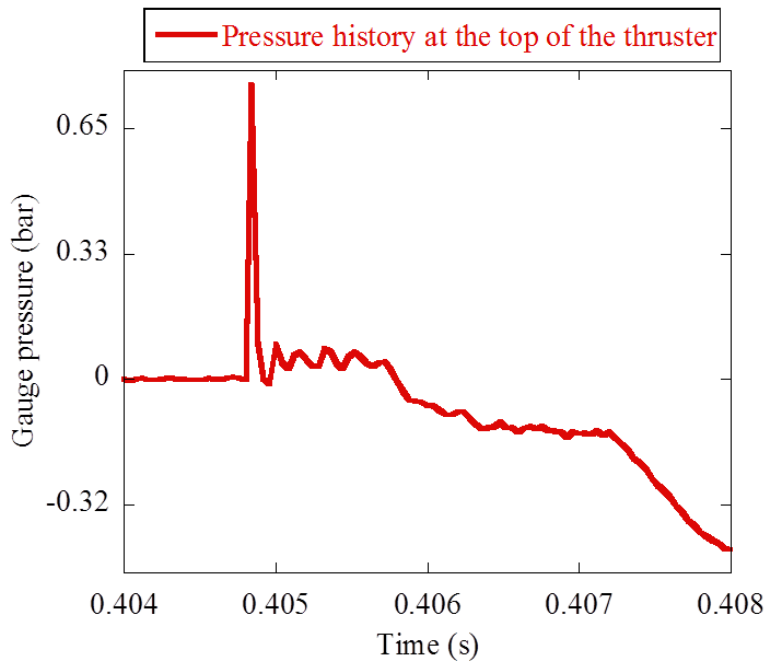


Figure 3.30. Pressure History in Case of Insulator Attachment (Pulse Count: Fifth)

Chapter 4

Conclusion

4.1 Improvement of Thrust Performance by Ti-Taper Reed Valve

New reed valve, Ti-taper reed valve, was designed and tested in the experiment. Compared to SUS304CSP reed valve, refilling volume was increased and partial filling rate was 1.7 higher than SUS304CSP reed valve. As a matter of course, plastic deformation did not be occurred. Furthermore, the increment ratio of propagation velocity of shockwave was smaller than the thruster without reed valve and it was found that plateau pressure time was longer. Hence, it can be said that the thrust was increased by attaching reed valve.

The thrust was verified by comparing with or without reed valve. When the thruster without reed valve was used, the thrust continued to be increased until around 15 % duty cycle. In contrast, the thruster with two-stage reed valve was used, the thrust continued to be increased until around 10 % duty cycle. The maximum thrust of the thruster with two-stage reed valve was about same to that of the thruster without reed valve. It means that the thrust decrement was prevented by attaching reed valve to the thruster in low duty cycle area and C_m was increased. In short, Ti-taper reed valve has an effect of increasing the thrust for Microwave Rocket.

4.2 Anomalous Ignition and Design Guide of Future Thruster

In this experiment, anomalous ignition which is the biggest reason for thrust decrement was occurred in high duty cycle. The reason of anomalous ignition which was occurred over 100 Hz repetitive pulse frequency in past study was that a lot of electrons remain due to the decrement of refilling time. In addition to this, the edges of reed valve and acrylic window attachment inside the thruster were cause in this experiment.

As mentioned above, the biggest reason of thrust decrease is anomalous ignition. Therefore, the thruster which does not generate anomalous ignition has to be made in the future. Although the number of reed valves is different, high pressure was generated at the top of the thruster by replacing metal attachment to insulator attachment. Therefore, the edges of metal should not be set inside the thruster and various attachments should be an insulator inside the thruster in future thruster.

If anomalous ignition is prevented completely, Ti-Taper reed valve has a higher effect to thrust increment and it is possible to increase duty cycle which maximum thrust is generated.

References

- [1] Koelle,D., 'Specific transportation costs to GEO-past, present and future', *Acta Astronautica*, **2003**, 53, 797-803
- [2] Saito, Y.; Yamashiro, R. & Ohkubo, S., 'The Vision for Next Flagship Launch Vehicle of Japan',*The 26th International Symposium on Space Technology and Science*, **2008**
- [3] SAITO, Y.; FUJITA, T.; YOSHIDA, H. & MORI, M., 'Overview of Studies on Space Solar Power Systems of JAXA', *Uchu Kagaku Gijutsu Rengo Koenkai Koenshu*, **2006**, 50, 3H05
- [4] Kantrowitz, A., 'Propulsion to orbit by ground-based lasers', *Astronautics & Aeronautics*,, **1972**,10, 74
- [5] Raizer Y.P., 'Laser-Induced Discharge Phenomena', *Consultants Bureau, New York and london*, **1977**,Ch.6
- [6] Myrabo, L., 'World record flights of beam-riding rocket lightcraft: Demonstration of 'disruptive' propulsion technology', *AIAA paper*, **2001**, 3798
- [7] Katsurayama, H.; Komurasaki, K.; Momozawa, A. & Arakawa, Y., 'Numerical and Engine Cycle Analyses of a Pulse Laser Ramjet Vehicle', *Transactions of Space Technology Japan*, **2003**, 1, 9-16
- [8] Katsurayama, H.; Komurasaki, K. & Arakawa, Y., 'A preliminary study of pulse-laser powered orbital launcher' *Acta Astronautica*, **2009**, 65, 1032-1041
- [9] Katsurayama, H.; Komurasaki, K. & Arakawa, Y., 'Feasibility for the orbital launch by pulse laser propulsion', *J Space Technol Sci*, **2005**, 20, 32-42
- [10] Endo, T.; Kasahara, J.; MATSUO, A.; IBANA, K.; SATO, S. & FUJIWARA, T., 'Pressure history at the closed end of a simplified pulse detonation engine', *AIAA journal, American Institute of Aeronautics and Astronautics*, **2004**, 42, 1921-1930
- [11] Sakamoto, K.; Kasugai, A.; Takahashi, K.; Minami, R.; Kobayashi, N. & Kajiwara, K., 'Achievement of robust high-efficiency 1 MW oscillation in the hard-self-excitation region by a 170 GHz continuous-wave gyrotron', *Nature physics*, **2007**, 3, 411-414
- [12] Sakamoto, K.; Kasugai, A.; Kajiwara, K.; Takahashi, K.; Oda, Y.; Hayashi, K. & Kobayashi, N., 'Progress of high power 170 GHz gyrotron in JAEA', *Nuclear Fusion*, **2009**, 49, 095019
- [13] Shiraishi, Y., 'Dependency of thrust performance on thruster length and beam conditions for Microwave Rocket', *Graduate School of Frontier Sciences, The University of Tokyo*, **2009**
- [14] Fukunari, M.; Yamaguti, T; Komatsu, R; Katsurayama, H; Komurasaki, K; Arakawa, Y, 'Preliminary Study on Microwave Rocket Engine Cycle', *Plasma Application and Hybrid Functionally Materials*, 20, 75, **2008**
- [15] Saitoh, S., 'Performance Evaluation of Reed Valve Air-Breathing System for Microwave Rocket', *Graduate School of Frontier Sciences, The University of Tokyo*, **2013**

- [16] Oda, Y., 'Application of Atmospheric Millimeter Wave Plasma to Rocket Propulsion', *Graduate School of Frontier Sciences, The University of Tokyo*, **2008**
- [17] Oda, Y.; Shibata, T.; Komurasaki, K.; Takahashi, K.; Kasugai, A. & Sakamoto, K., 'Thrust Performance of a Microwave Rocket under Repetitive-Pulse Operation', *JOURNAL OF PROPULSION AND POWER*, **2009**, 25, 118-122
- [18] Shiraishi, Y.; Oda, Y.; Shibata, T.; Komurasaki, K.; Takahashi, K.; Kasugai, A. & Sakamoto, K., 'Air Breathing Processes in a Repetitively Pulsed Microwave Rocket', *AIAA-2008-1085, 46th AIAA Aerospace Sciences Meeting and Exhibit, Reno, Nevada, Jan. 7-10, 2008, 1085*
- [19] Oda, Y.; Komurasaki, K.; Takahashi, K.; Kasugai, A. & Sakamoto, K., 'An Experimental Study on a Thrust Generation Model for Microwave Beamed Energy Propulsion', *AIAA-2006-765, 44th AIAA Aerospace Sciences Meeting and Exhibit, Reno, Nevada, Jan. 9-12, 2006, 1, 1-1*
- [20] Matsuo, K. '圧縮性流体力学 内部流れの理論と解析', 理工学社, **1994**

修士論文に関わる学会発表リスト

学会での受賞歴

優秀発表賞

- [1] ○栗田哲志、齋藤翔平、福成雅史、山口敏和、小紫公也（東京大学）、小田靖久、梶原健、高橋幸司、坂本慶司（日本原子力研究開発機構）「マイクロ波ロケットの繰り返しパルス周波数限界の向上」、『第56回宇宙科学技術連合講演会』、P35、別府、2012年11月

国際会議での発表（第一著者1件、共著1件、うち2件は予定）

- [2] *Satoshi Kurita (The University of Tokyo), "Repetitive Pulse Frequency Limitation of Microwave Rocket in Launch Experiment", '29th International Symposium on Space Technology and Science', 2013-s-61-b, Nagoya, Japan. (Jun.2013)
- [3] *M. Fukunari, T.Yamaguchi, S.Saitoh, K.Asai, S.Kurita, Komurasaki K (The University of Tokyo), Y. Oda, K.Kajiwara, K.Takahashi, K.Sakamoto (Japan Atomic Energy Agency), "Thrust Performance and Plasma Generation of Microwave Rocket with Microwave Beam Space Transmission System", 'IEEE Pulsed Power and Plasma Science Conference 2013', 6F-4, California, US. (Jun.2013)
- [4] *Masafumi Fukunari, Toshikazu Yamaguchi, Kenta Asai, Satoshi Kurita, Nat Wongsuryat and Kimiya Komurasaki (The university of Tokyo), Yasuhisa Oda, Ryosuke Ikeda, Ken Kajiwara, Koji Takahashi and Keishi Sakamoto (Japan Atomic Energy Agency), "Launch Experiment and Thrust Measurement of a Kg-order Microwave Rocket", 'Asian Joint Conference on Propulsion and Power 2014', Jeju Island, Korea.(March.2014)
- [5] *Masafumi Fukunari, Toshikazu Yamaguchi, Kenta Asai, Satoshi Kurita, Nat Wongsuryat and Kimiya Komurasaki (The university of Tokyo), Yasuhisa Oda, Ryosuke Ikeda, Ken Kajiwara, Koji Takahashi and Keishi Sakamoto (Japan Atomic Energy Agency), "Microwave Rocket with quasi-optical microwave power transmission system and flight demonstration", 'International High Power Laser Ablation and Beamed Energy Propulsion', Santa Fe, US.(April.2014)

国内学会での発表（第一著者2件、共著2件）

- [6] ○栗田哲志、齋藤翔平、福成雅史、山口敏和、小紫公也（東京大学）、小田靖久、梶原健、高橋幸司、坂本慶司（日本原子力研究開発機構）「マイクロ波ロケットの繰り返しパルス周波数限界の向上」、『第56回宇宙科学技術連合講演会』、P35、別府、2012年11月（上記優秀発表賞）

- [7] ○栗田哲志、齋藤翔平、福成雅史、山口敏和、小紫公也（東京大学）、小田靖久、梶原健、高橋幸司、坂本慶司（日本原子力研究開発機構）「垂直打ち上げ実験に向けたマイクロ波ロケットのリード弁式吸気機構の改善」、『第 53 回航空原動機・宇宙推進講演会』、JSASS-2013-0036、倉敷、2013 年 3 月
- [8] ○齋藤翔平、浅井健太、栗田哲志、福成雅史、山口敏和、小紫公也（東京大学）、小田靖久、梶原健、高橋幸司、坂本慶司（日本原子力研究開発機構）「kg 級マイクロ波ロケットの打ち上げ実証実験報告」、『平成 24 年度宇宙輸送シンポジウム』、STEP-2012-034、相模原、2013 年 1 月
- [9] ○福成雅史、山口敏和、齋藤翔平、浅井健太、栗田哲志、小紫公也（東京大学）、小田靖久、梶原健、高橋幸司、坂本慶司（日本原子力研究開発機構）、「リード弁式吸気機構によるマイクロ波ロケットの推力性能改善」、『第 45 回流体力学講演会/航空宇宙数値シミュレーション技術シンポジウム 2013』、IC04、船堀、2013 年 7 月